Geologica Acta, Vol.9, Nos 3-4, September - December 2011, 265-272
DOI: 10.1344/105.000001698
Available online at www.geologica-acta.com

geologica acta

U-Pb Geochronology of detrital zircons from the Venezuelan passive margin: implications for an Early Cretaceous Proto-Orinoco river system and Proto-Caribbean ocean basin paleogeography

M.I. NOGUERA [1] [2] **J.E. WRIGHT** [1] [*] **F. URBANI** [3] **J. PINDELL** [4]

[1] **Department of Geology, University of Georgia**
Athens, GA 30602

[2] **Current address: Swift Energy Operating, LLC**
16825 Northchase Drive, Suite 400, Houston, TX 77060

[3] **FUNVISIS, El Llanito and Universidad Central de Venezuela, Escuela de Geología**
Final Calle Mara, Caracas, Venezuela

[4] **Department of Earth Science, Rice University Keith-Weiss Geological Laboratory**
6100 Main Street, Houston, TX 77005 and Tectonic Analysis Ltd., Chestnut House, Burton Park, Duncton, West Sussex, GU28 0LH, England

[*] Corresponding author: James E. Wright, Jwright@gly.uga.edu, phone: 706-542-4394, fax: 706-542-2425

ABSTRACT

The Guyana Shield has long been interpreted as the source of siliciclastic detritus within the Cretaceous passive margin strata of northern Venezuela. We have determined U-Pb ages of detrital zircons separated from Early Cretaceous strata of the passive margin. Although the Guyana shield is the probable source for much of the Archean, Paleoproterozoic and early Mesoproterozoic detrital zircon grains, there is a prominent age population (ca.0.95-1.2Ga) that is not easily explained as being derived from the shield. A western source in the Venezuelan and/or northern Colombian Andes is suggested for this detrital component. We propose that a Proto-Orinoco river system drained both the Guyana Shield and the Venezuelan and Colombian Andes and that branches of this river system were funneled through Triassic/Jurassic rift basins that formed during initial opening of the Proto-Caribbean Seaway. The detrital zircon age data have implications for paleogeographic reconstructions of the Caribbean region prior to the breakup of Pangea and the longevity of continental scale river systems.

KEYWORDS | **Detrital Zircon. Passive Margin. Venezuela.**

INTRODUCTION

The provenance of sandstones as determined by U-Pb detrital zircon geochronology has become a widely used tool in global plate tectonic reconstructions. For example, it has been used to help reconstruct Pangea in the Caribbean region prior to the opening of the Proto-Caribbean as a number of detrital zircon investigations have suggested a northern South American provenance for Paleozoic strata now found in Mexico (e.g. Weber et al., 2006, 2008; Ortega-Obregon et al., 2009). In addition, currently geographically dispersed Jurassic to Cenozoic sediments of the Caribbean region are interpreted to have been derived from northern Venezuela (e.g. Rojas-Agramonte et al., 2008; Pindell et al., 2009). However, there are no published U-Pb detrital zircon provenance studies for the northern South American margin to test these hypotheses yet. We report the first U-Pb detrital zircon ages from the passive margin of Venezuela in order to establish a provenance barcode that can be used to quantitatively assess Pangean paleogeography in this region.

In addition, a number of detrital zircon investigations have been used to provide evidence for the presence and/or location of continental scale paleofluvial drainage systems (Riggs et al., 1996; Dickinson and Gehrels, 2003; Prokopiev et al., 2008). Our data, in conjunction with previous investigations, clearly identifies such a system that operated in northern South America.

GEOLOGICAL SETTING

Separation of North and South America during the breakup of western Pangaea created the Proto-Caribbean seaway and resulted in the establishment of an Early Cretaceous passive margin in northern Venezuela. During the Triassic and Jurassic, continental breakup led to formation of numerous rift basins that were filled with continental red beds and associated volcanic rocks (Yoris et al., 1997; Ramos, 2009). Although rocks associated with the early rifting phase of passive margin development are exposed in western Venezuela (Perijá and Mérida Andes) where they attain a thickness of 300 to 3400m (Schubert, 1986), in central and eastern Venezuela these deposits are buried by younger strata and are known only from drill hole data (Feo-Codecido et al., 1984). For example, the Espino Graben (Fig. 1) is a buried rift basin that trends WSW-ENE across northern Venezuela and is known from wells to contain as much as 1.5km of Jurassic red beds and volcanic rocks dated at 162Ma (Feo-Codecido et al., 1984; Motiscka, 1985; Rodríguez and Rodríguez, 2003).

The Triassic-Jurassic rifting phase was followed by the development of an Early Cretaceous passive margin dominated by siliciclastic sedimentation above a regional transgressive peneplain. Regional transgression onto the subsiding passive margin led to onlap of continental to shallow marine facies, followed by deeper water facies which reached a maximum in the Late Cretaceous (Turonian-Coniacian) and is reflected in the Cretaceous stratigraphic record by a gradual change from siliciclastic dominated sedimentation in the Early Cretaceous to more pelagic shale and carbonate sedimentation in the Late Cretaceous (Pindell and Erikson, 1994).

We have obtained a total of 560 detrital zircon analyses from six samples of siliciclastic Early Cretaceous passive-margin units along northern Venezuela (Fig. 1). Sample locations and analytical data are contained in the supplementary files.

PASSIVE MARGIN SAMPLES

Four Early Cretaceous stratigraphic units (six samples) of the Venezuelan passive margin were sampled for detrital zircon dating (Fig. 1). The stratigraphic terminology of the passive margin strata of northern Venezuela varies from west to east. The samples for this study were collected from the Early Cretaceous Aguardiente (westernmost unit sampled), Bobare, Araure and Barranquín (easternmost unit sampled) formations.

A single sample of quartz arenite was collected from the Aguardiente Formation (Barremian-Aptian) which contains quartz-rich sandstones with local glauconitic sandstone and limestone beds and is interpreted to have been deposited in a shallow marine deltaic setting (Salvador, 1961).

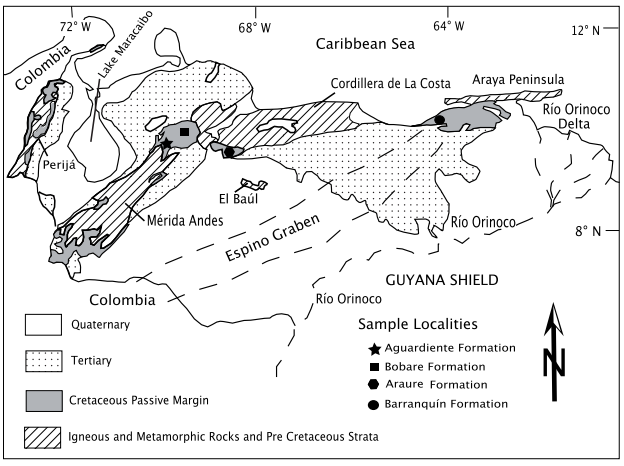

FIGURE 1 | **Simplified geologic map of northern Venezuela showing the location of Early Cretaceous passive margin samples collected for this study.**

Two samples of quartz arenite were analyzed from the Bobare Formation (Barremian-Albian) of northwestern Venezuela. Bellizzia and Rodríguez (1967) described the unit as being composed of massive, sometimes conglomeratic, quartz-rich-sandstone, shale and siltstone and interpreted the Bobare to have been deposited in an unstable shelf environment.

One sample of a schistose quartz-sandstone from the Araure Formation (Neocomian-Barremian?) was collected. Renz and Short (1960) and Bushman (1967) described the unit as containing thick conglomerate layers, alternating with arkosic sandstone, quartz sandstone and silty shales; it is interpreted to have been deposited in continental to shallow marine waters.

Two samples (quartz arenites and sublitharenites) were sampled for zircons and analyzed from the Barranquín Formation (Barremian-Aptian) of eastern Venezuela. The unit is composed of quartz sandstone, intercalated with shale and occasional limestone, and is considered to have been deposited in deltaic to internal inner shelf (bar) environments (Pindell and Erikson, 1994; Erikson and Pindell, 1998a, b).

ANALYTICAL METHODS

U-Pb geochronology of zircons was conducted by laser ablation multicollector inductively coupled plasma mass spectrometry (LA-MC-ICPMS) at the Arizona LaserChron Center. Analytical protocols followed Gehrels et al., 2006. The analyses involve ablation of zircon with a New Wave/Lambda Physik DUV193 Excimer laser (operating at a wavelength of 193nm) using a spot diameter of 30microns. The ablated material is carried in helium into the plasma source of a GVI Isoprobe, which is equipped with a flight tube of sufficient width that U, Th, and Pb isotopes are measured simultaneously. All measurements are made in static mode, using 10^{11} ohm Faraday detectors for ^{238}U, ^{232}Th, ^{208}Pb, and ^{206}Pb, a 10^{12} ohm faraday collector for ^{207}Pb, and an ion-counting channel for ^{204}Pb. Ion yields are ~1.0mv per ppm. Each analysis consists of one 12-second integration on peaks with the laser off (for backgrounds), 12 one-second integrations with the laser firing, and a 30 second delay to purge the previous sample and prepare for the next analysis. The ablation pit is ~12 microns in depth. For each analysis, the errors in determining $^{206}Pb/^{238}U$ and $^{206}Pb/^{204}Pb$ result in a measurement error of ~1-2% (at 2-sigma level) in the $^{206}Pb/^{238}U$ age. The errors in measurement of $^{206}Pb/^{207}Pb$ and $^{206}Pb/^{204}Pb$ also result in ~1-2% (at 2-sigma level) uncertainty in age for grains that are >1.0Ga, but are substantially larger for younger grains due to low intensity of the ^{207}Pb signal. For most analyses, the cross-over in precision of $^{206}Pb/^{238}U$ and $^{206}Pb/^{207}Pb$ ages occurs at 0.8-1.0Ga. Common Pb correction is accomplished by using the measured ^{204}Pb and assuming an initial Pb composition from Stacey and Kramers (1975) (with uncertainties of 1.0 for $^{206}Pb/^{204}Pb$ and 0.3 for $^{207}Pb/^{204}Pb$). Our measurement of ^{204}Pb is unaffected by the presence of ^{204}Hg because backgrounds are measured on peaks (thereby subtracting any background ^{204}Hg and ^{204}Pb), and because very little Hg is present in the argon gas. Inter-element fractionation of Pb/U is generally ~20%, whereas apparent fractionation of Pb isotopes is generally ~2%. In-run analysis of fragments of a large zircon crystal (generally every fifth measurement) with known age of 564±4Ma (2-sigma error) is used to correct for this fractionation. The uncertainty resulting from the calibration correction is generally 1-2% (2-sigma) for both $^{206}Pb/^{207}Pb$ and $^{206}Pb/^{238}U$ ages. The analytical data are reported in the supplementary document files. Uncertainties shown in these tables are at the 1-sigma level, and include only measurement errors. Interpreted ages are based on $^{206}Pb/^{238}U$ for <1000Ma grains and on $^{206}Pb/^{207}Pb$ for >1000Ma grains. This division at 1000Ma results from the increasing uncertainty of $^{206}Pb/^{238}U$ ages and the decreasing uncertainty of $^{206}Pb/^{207}Pb$ ages as a function of age. The resulting interpreted ages are shown on relative age-probability diagrams (from Ludwig, 2003). These diagrams show each age and its uncertainty (for measurement error only) as a normal distribution, and sum all ages from a sample into a single curve.

We obtained 560 U-Pb zircon ages (Supplementary Data), derived from six samples of four Early Cretaceous passive margin formations of northern Venezuela.

PROVENANCE OF THE EARLY CRETACEOUS PASSIVE MARGIN

Previous investigations interpreted the Early Cretaceous siliciclastic passive margin strata to have been derived entirely from the Guyana Shield to the south (van Andel, 1958; González de Juana et al., 1980), with few indications of any particular drainage systems. The ages of detrital zircons from the passive margin units range from late Archean (2731Ma) to Silurian (415Ma), and all samples display similar distribution patterns with the exception of the Araure Formation (Fig. 2). The data are similar to U-Pb detrital zircon ages obtained from the modern Orinoco River and its tributaries which drain the northern Andes of Colombia and Venezuela as well as the Guyana Shield (Goldstein et al., 1997). Prominent Precambrian age peaks in the passive margin samples occur at ca.2.0, 1.8, 1.4 to 1.6, and 1.2- 0.95Ga. There are also a few grains that gave

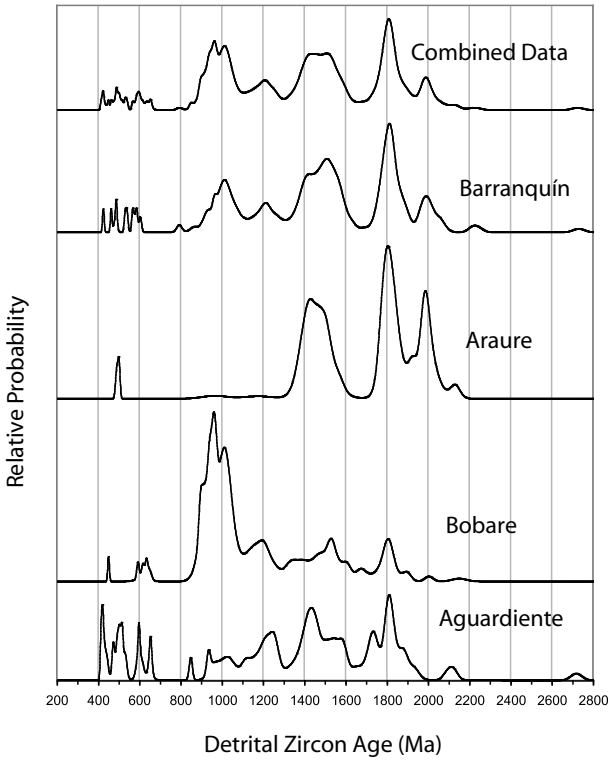

FIGURE 2 | **Probability density plot of U-Pb zircon detrital zircon ages from Early Cretaceous passive margin samples.**

late Archean ages. In addition, about 6 percent of the grains fall into the ca. 400-650Ma age range.

The Archean, Paleoproterozoic, and early Mesoproterozoic detrital zircon populations are a good match to known age provinces in the Guayana Shield (Fig. 3). Archaen rocks are present in the Imataca Complex of the Central Amazonian Province, and age peaks of ca.1.8 and 2.0Ga plus a few grains of ca.2.1 and 2.2Ga are a good match to the Maroni-Itacaiunal, Ventuari-Tapajos and Río Negro-Jurena Provinces (Fig. 3). The ca. 1.5Ga age peak is most likely derived from Rapakivi granites, including the 30,000km^2 Parguaza Batholith, which intrude older rocks of the Amazonia Craton (Gaudette et al., 1978; Mendoza, 1978, 2005), especially within the Ventuari-Tapajos Province.

The most remarkable feature of our dataset is the large proportion of detrital zircons giving prominent peaks at ca. 1.2 and 0.95-1.1Ga. The only known southern source area for this age population is the Sunsas province that lies far to the south in the Amazonian craton of Bolivia (Fig. 3). Rocks of this age, however, are also known from the basement inliers of the northern Andes of Colombia (Santa Marta, Santander, and Garzón massifs; e.g. Kroonemberg, 1982; Restrepo-Pace et al., 1997; Cordani et al., 2005; Fig. 3) and may also be present in the Mérida Andes (Figs. 1, 3; Burkley, 1976). Paleozoic strata from these areas are also a potential source for detrital zircons but there are no published data to evaluate that possibility. We speculate that the ca. 0.95-1.2Ga age population of detrital zircon was derived from the basement rocks of Colombia and possibly the Mérida Andes, and their Paleozoic cover, rather than the Sunsas Province senso stricto. The paleogeographic implications of this interpretation are discussed below.

There are several potential source areas for the Paleozoic and late Neoproterozoic detrital populations (ca. 415-650Ma) which only account for approximately 6 percent of the total number of analyses. The Neoproterozoic Brasiliano and Pampean Provinces contain ages ranging from ca. 0.7-0.5Ga, and the Famatinian arc terrane is a potential source terrane for zircons in the 0.5-0.4Ga age range (Fig. 3). These provinces are, however, located extremely far from the Early Cretaceous passive margin of Venezuela. Other potential source regions exist in the Mérida Andes and the Perijá Range (Fig. 2). These areas are uplifted blocks that contain Paleozoic and Precambrian rocks overlain by Cretaceous passive margin strata. In addition, the Cordillera de la Costa Belt of northern Venezuela and the northern Colombian Andes are possible source regions for this detrital population. The older rocks in all of these areas probably represent windows into the crust that underlies much of the Llanos Cenozoic foreland to the Colombian and Venezuelan thrustbelts (Feo-Codecido et al., 1984; Fig. 1). Unfortunately, little modern geochronology has been done in these regions. In the Cordillera de la Costa area (Fig. 1) Sisson et al. (2005) reported early Paleozoic (Cambrian and Ordovician) U-Pb zircon ages from several granitoid intrusions. Urbani et al. (2007) also reported a Cambrian (508Ma) U-Pb zircon age from the Todasana metadiorite located in the Cordillera de la Costa belt. Viscarret et al. (2007) reported early Paleozoic (Cambro/Ordovician) as well as late Paleozoic (Permian) U-Pb zircon ages determined on volcanic and plutonic rocks from the El Baúl area (Fig. 1). Burkley (1976) carried out an extensive U-Pb zircon geochronology project in the Mérida Andes. Although all his samples are complicated by Pb loss and/or the presence of inherited older zircon, he was able to determine early Paleozoic ages (Devonian, Silurian and Ordovician) on a number of granitoid bodies as well as some late Neoproterozoic ages of ca. 600Ma from three other granitoid intrusions. Thus, a local Venezuelan source region is a possibility for this detrital component. Paleozoic strata of Colombia and the Mérida Andes of Venezuela are also a potential source region for this detrital population, but no detrital zircon geochronology exists for these rock units.

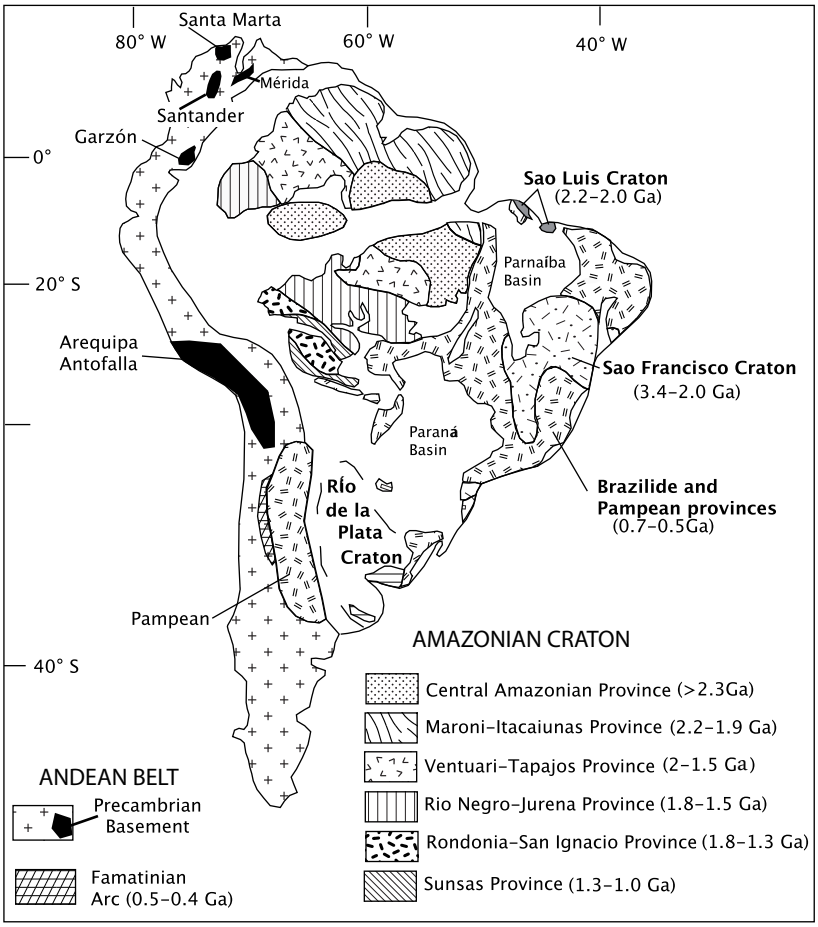

FIGURE 3 | **Generalized geologic map of the South American cratons depicting major tectonic provinces. Modified from Cordani et al. (2000) and Tassinari et al. (2000).**

PALEOGEOGRAPHIC IMPLICATIONS FOR THE PASSIVE MARGIN OF VENEZUELA

The modern Orinoco river system drains both the Guyana Shield and the Andes of Colombia and Venezuela and contains a population of detrital zircons that is similar to our Early Cretaceous passive margin samples, including the prominent ca. 0.95-1.2Ga population (Goldstein et al., 1997). Kasper and Larue (1986) attributed the great thickness of Paleocene and Eocene clastic detritus in the Lake Maracaibo Basin (Fig. 1) to a north-flowing paleofluvial system that drained the Colombian Andes and Guyana shield regions which they called the Proto-Orinoco River. In addition, Hoorn et al. (1995) likewise came to the conclusion that a northwest-flowing Proto-Orinoco River system drained the Andes and the Guyana shield prior to the Late Miocene forming a delta in the Lake Maracaibo region. By the Middle Miocene, uplift in Colombia and the Mérida Andes of Venezuela is postulated to have deflected the paleofluvial system into a more east-west orientation, marking the beginning of the current Orinoco drainage (Díaz de Gamero, 1996).We suggest that a similar Proto-Orinoco river system was responsible for the detrital zircon provenance of the Early Cretaceous passive margin of Venezuela. Our sample localities are shown in Figure (4A) in relation to the Jurassic Espino and Uribante rift structures. Note that the deltaic to shallow shelf deposits of the Barranquín formation occur on strike with the Espino Graben, and the Aguardiente and Bobare sample collection sites lie above the Uribante rift. We suggest that a paleo-river system drained eastern Colombia and western Venezuela and flowed down broad valleys above both the Espino Graben and Uribante rifts, following the principal that rifts are where subsidence is greatest, thus supplying the 0.95-1.2Ga detrital zircon component (Fig. 4A) before and during initial marine transgression in these areas.

REGIONAL PALEOGEOGRAPHIC IMPLICATIONS

Rojas-Agramonte et al. (2008) analysed 19 detrital zircon grains from the clastic sediments of the Early (?) to Late Jurassic (Oxfordian) San Cayetano Formation of western Cuba. The San Cayetano Formation is considered

to have been deposited in and above rift basins developed during breakup of Pangea during initial opening of the Proto-Caribbean (Pindell, 1985; Martön and Buffler, 1994, 1999; Iturralde-Vinent, 2003). Although a number of possible source areas have been suggested (including a Laurentian source), Rojas-Agramonte et al. (2008) concluded from their detrital zircon data that the San Cayetano Formation most likely had a Gondwanan (South American) provenance. They further speculated that the basin was geographically located off the current northeastern Venezuelan margin near the termination of the Espino Graben (Fig. 4B) and that it was fed in part by a river system running through the Espino and Uribante rifts. Although not explicitly discussed in their paper, the occurrence of a ca.1.5-1.6Ga detrital zircons in the San Cayetano Formation strongly supports a South American provenance as this age range lies within the Laurentian magmatic gap but is a prominent age found within the Amazonian craton as previously discussed and as shown by our detrital zircon data (Fig. 2). Also, their data (albeit very limited) exhibit very similar age populations to those of the Venezuelan passive margin strata in support of their general paleogeographic model. It thus appears that the Espino Graben and Uribante rifts hosted a Jurassic to Early Cretaceous Proto-Orinoco river system.

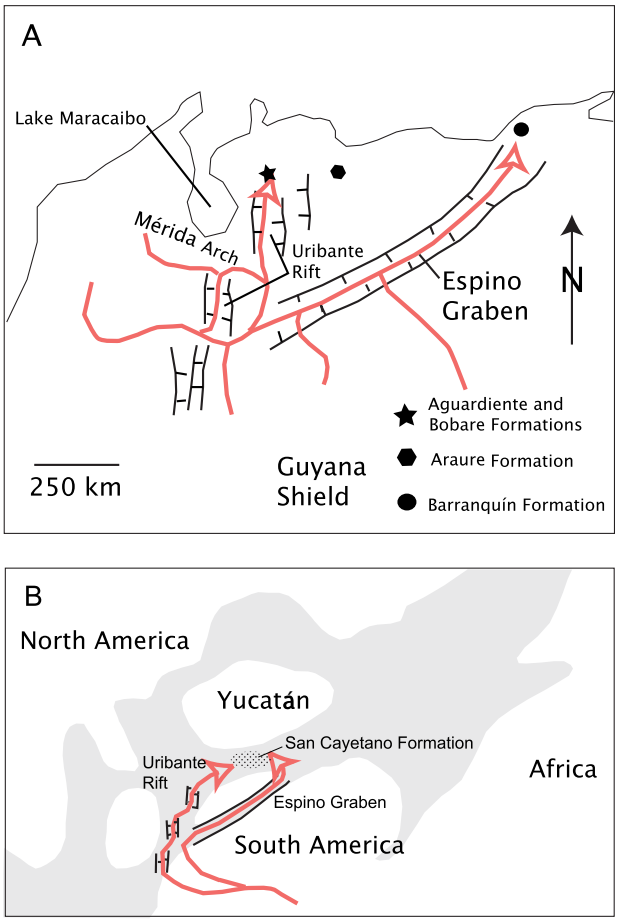

FIGURE 4 | **A) Proposed paleogeography of northern Venezuela depicting the Early Cretaceous Proto-Orinoco river drainage system. Arrows indicate possible sedimentary transport along a Proto-Orinoco river system. B) Paleogeography of the San Cayetano Formation as proposed by Rojas-Agramonte et al. (2008). Gray areas denote highly extended continental crust. The figure is adapted from Pindell and Kennan (2001) and Rojas-Agramonte et al. (2008).**

The paleofluvial system postulated here for the Jurassic and Early Cretaceous marked the beginning of a continental-scale drainage system that was resumed, after middle Cretaceous drowning of the paleo-river valleys (Villamil and Pindell, 1998), in the Paleogene, when the Caribbean collisional foredeep was first imposed on the western reaches of the northern South American passive margin (Pindell et al., 1998). It continues today as the Orinoco river, after a long history of persistent eastward deflection along the Venezuela-Trinidad margin due to the eastward-younging oblique collision of the Caribbean Plate and associated eastward lengthening of the zone of orogenic uplift (Díaz de Gamero, 1996). Thus, the continental scale Orinoco fluvial system seems to have persisted since the initial formation of the northern South American passive margin during the breakup of Pangea, suggesting that the longevity of such river systems may be the same order of magnitude as that of plate boundaries (eg. Prokopiev et al., 2008).

ACKNOWLEDGMENTS

This paper is a contribution to the BOLIVAR project supported by NSF grants EAR 0607533 and 0087361 to Wright, and support from NSF EAR-0003572 is acknowledged by Pindell. The GEODINOS project (Fundación Venezolana de Investigaciones Sismológicas and Universidad Central de Venezuela) provided logistical support in the field. Noguera received grant support from AAPG, the University of Georgia, Miriam Watts–Wheeler Scholarship Fund, and the Latin American and Caribbean Studies Institute at the University of Georgia. University of Georgia undergraduate students Ted Lord, Emily First, Auggie Parinello and Corin Steadman helped with mineral spearation and/or the LA-MC-ICPMS analyses. Student travel and LA-MC-ICPMS analyses were subsidized by the Arizona LaserChron center through NSF grants EAR 0443387 and 0732436.

REFERENCES

Bellizzia, A., Rodríguez, D., 1967. Excursión a la región de Duaca–Barquisimeto–Bobare. Caracas, Boletín de Geología, 16, 289-309.

Burkley, L.A., 1976. Geochronology of the Central Andes, Venezuela. Doctoral Thesis. Cheveland (Ohio), Case Western Reserve University, 159pp.

Bushman, J.R., 1967. Geología de la región de Agua Blanca y San Carlos, Venezuela. Caracas, Boletín de Geología, 16, 311-336.

Cordani, U.G., Sato, K., Teixeira, W., 2000. Crustal evolution of the South American platform. In: Cordani, U.G., Milani, E.J., Filho, A.T. (eds.). Tectonic evolution of South America. Rio de Janeiro, 31st International Geological Congress, 19-40.

Cordani, U., Cardona, A., Jiménez, D.M., 2005. Geochronology of Proterozoic basement inliers in the Colombian Andes: tectonic history of remnants of a fragmented Grenville belt. In: Vaughan, A.P.M., Leat, P.T., Pankhurst, R.J. (eds.). Terrane Processes of the Margins of Gondwana. London, Geological Society, 246 (Special Publications), 329-346.

Díaz de Gamero, M.L., 1996. The changing course of the Orinoco River during the Neogene: a review. Paleogeography, Paleoclimatology, Palaeoecology, 123, 385-402.

Dickinson, W.R., Gehrels, G.E., 2003. U-Pb ages of detrital zircons from Permian and Jurassic eolian sandstones of the Colorado Plateau, USA: Paleogeographic implications. Sedimentary Geology, 163, 29-66.

Erikson, J.P., Pindell, J.L., 1998a. Cretaceous through Eocene sedimentation and Paleogeography of a Passive Margin in northeastern Venezuela. In: Pindell, J.L., Drake, C.L. (eds.). Paleogeographic Evolution and Non-Glacial Eustasy, Northern South America. Society for Sedimentary Geology (SEPM), 58 (Special Publications), 218-259.

Erikson, J.P., Pindell, J.L., 1998b. Sequence stratigraphy and relative sea-level history of the Cretaceous to Eocene passive margin of North-East Venezuela and the possible tectonic and eustatic causes of stratigraphic development. In: Pindell, J.L., Drake, C.L. (eds.). Paleogeographic Evolution and Non-Glacial Eustasy, Northern South America. Society for Sedimentary Geology (SEPM), 58 (Special Publications), 261-281.

Feo-Codecido, G., Smith, F.Jr., Aboud, N., Di Giacomo, E., 1984. Basement and Paleozoic rocks of the Venezuelan Llanos Basin. Geological Society of America Memoir, 162, 175-187.

Gaudette, H.E., Mendoza, V., Hurley, F.M., 1978. Geology and age of the Parguaza Rapakivi Granite, Venezuela. Geological Society of America Bulletin, 89, 1135-1340.

Gehrels, G.E., Valencia, V., Pullen, A., 2006. Detrital zircon geochronology by laser-ablation multicollector ICPMS at the Arizona Laser-Chron Center. In: Olszewski, T., Huff, W. (eds.). Geochronology: Emerging opportunities. Philadelphia, Paleontological Society Short Course, 1-10.

Goldstein, S.L., Arndt, N.T., Stallard, R.F., 1997. The history of a continent from U-Pb ages of zircons from Orinoco River sand and Sm-Nd isotopes in Orinoco basin river sediments. Chemical Geology, 139, 271-286.

González de Juana, C., Iturralde, J.M., Piccard, X., 1980. Geología de Venezuela y de sus Cuencas Petrolíferas. Caracas, Foninves, 1031pp.

Hoorn, C., Guerrero, J., Sarmiento, G.A., Lorente, M.A., 1995. Andean tectonics as a cause for changing drainage patterns in Miocene northern South America. Geology, 23, 237-240.

Iturralde-Vinent, M.A., 2003. A brief account of the evolution of the Caribbean seaway: Jurassic to present. In: Prothero, D., Ivany, L., Nesbitt, E., (eds.). From greenhouse to icehouse: The marine Eocene–Oligocene transition. New York, Columbia University Press, 386-396.

Kasper, D.A., Larue, D.K., 1986. Paleogeographic and tectonic implications of quartzose sandstones of Barbados. Tectonics, 5, 837-854.

Kroonemberg, G.S., 1982. A Grenvillian granulite belt in the Colombian Andes and its relations to the Guyana Shield. Geologie en Mijnbouw, 61, 325-333.

Ludwig, K.R., 2003. Isoplot 3.00. Berkeley Geochronology Center, 4 (Special Publications), 70pp.

Marton, G., Buffler, R.T., 1994. Jurassic reconstruction of the Gulf of Mexico Basin. International Geology Review, 36, 545-586.

Marton, G., Buffler, R.T., 1999. Jurassic-Early Cretaceous tectono-paleogeographic evolution of the southeastern Gulf of Mexico Basin. In: Mann, P. (ed.). Caribbean Basins. Amsterdam, Elsevier Science, Series Sedimentary Basins of the World, 4, 63-91.

Mendoza, V., 1978. Petrogénesis del granito rapakivi del Parguaza, NO del Escudo de Guyana, Venezuela. Caracas, Boletín de Geología, 7(5) (Special Publications), 3549-3588.

Mendoza, V., 2005. Geología de Venezuela. Geos, 38, 119-123 and 783pp. in CD.

Moticska, P., 1985. Volcanismo Mesozoico en el subsuelo de la Faja Petrolífera de Orinoco. Caracas, Memoria VI Congreso Geológico Venezolano, 3, 1929-1943.

Ortega-Obregon, C., Keppie, J.D., Murphy, J.B., 2009. Geology and geochronology of Paleozoic rocks in western Acatlan Complex. Southern Mexico: Evidence for contiguity across an extruded high-pressure belt and constraints on Paleozoic reconstructions. Geological Society of America Bulletin, 121, 1678-1694.

Pindell, J.L., 1985. Alleghanian reconstruction and the subsequent evolution of the Gulf of Mexico, Bahamas, and Proto-Caribbean Sea. Tectonics, 4, 1-39.

Pindell, J.L., Erikson, J.P., 1994. Mesozoic passive margin of northern South America. In: Salfity, J.A. (ed.). Cretaceous tectonics in the Andes. Vieweg Publishing, Earth Evolution Sciences, International Monograph Series, 1-60.

Pindell, J.L., Higgs, R., Dewey, J.F., 1998. Cenozoic palinspastic reconstruction, paleogeographic evolution, and hydrocarbon setting of the northern margin of South America. In: Pindell, J.L., Drake, C.L. (eds.). Paleogeographic Evolution and Non-glacial Eustasy, northern South America. Tulsa, Society for Sedimentary Geology (SEPM), 58 (Special Publications), 45-86.

Pindell, J.L., Kennan, L.J.G., 2001, Kinematic evolution of the Gulf of Mexico and the Caribbean. In: Fillon, R. (ed.). Transactions, 21st Bob Perkins Gulf Coast Section of the Society of Economic and Paleontologists and Mineralogists (GCSSEPM) Research Conference, Gulf Coast Section of the Society of Economic and Paleontologists and Mineralogists, 193-220.

Pindell, J., Kennan, L., Wright, D., Erikson, J., 2009. Clastic domains of sandstones in central/eastern Venezuela, Trinidad and Barbados: heavy mineral and tectonic constraints on

provenance and palaeogeography. In: James, K.H., Lorente, M.A., Pindell, J.L. (eds.). The Origin and Evolution of the Caribbean Plate. London, Geological Society, 328 (Special Publications), 739-794.

Prokopiev, A.V., Toro, J., Miller, E.L., Gehrels, G.E, 2008. The paleo-Lena River-200 m.y. of transcontinental zircon transport in Siberia. Geology, 36(9), 699-702.

Ramos, V.A., 2009. Anatomy and global context of the Andes: Main geologic features and the Andean orogenic cycle. In: Kay, S.M., Ramos, V.A., Dickinson, W.R. (eds.). Backbone of the Americas: Shallow subduction, plateau uplift, and ridge and terrane collision. Geological Society of America Memoir, 204, 31-65.

Renz, O., Short, K.C., 1960. Estratigrafía de la región comprendida entre el Pao y Acarigua, estados Cojedes y Portuguesa. Caracas, Memoria III Congreso Geológico Venezolano, 1, 277-315.

Restrepo-Pace, P.A., Ruiz, J., Gehlers, G., 1997. Geochronology and Nd isotopic data of Grenville-age rocks in the Colombian Andes: new constraints for Late Proterozoic-Early Palezoic paleocontinental reconstructions of the Americas. Earth and Planetary Science Letters, 150, 427-441.

Riggs, N.R., Lehman, T.M., Gehrels, G.E., 1996. Detrital zircon link between headwaters and terminus of the Upper Triassic Chinle-Dockum paleoriver system. Science, 273, 97-100.

Rodríguez, I., Rodríguez, J., 2003. Gravity and magnetic modelling across the Guárico Sub-basin, Espino Graben, Venezuela. Institut de Recherche pour le développement (IRD) – Université Paul Sabatier, Andean Geodynamics, Extended Abstracts, 533-536.

Rojas-Agramonte, Y., Kroner, A., Pindell, J., 2008. Detrital zircon geochronology of Jurassic sandstones of western Cuba (San Cayetano Formation): Implications for the Jurassic paleogeography of the NW Proto-Caribbean. American Journal of Science, 308, 639-656.

Salvador, A., 1961. Guidebook to the geology of northeastern Trujillo. Maracaibo, Sociedad Venezolana de Geólogos, Region Occidental, 3, 33pp.

Schubert, C., 1986. Stratigraphy of the Jurassic La Quinta Formation, Mérida Andes, Venezuela: type sections. Zeitschrift der Deutsche Geologische Gesellschaft, 137, 391-411.

Sisson, V., Avé Lallemant, H.G., Ostos, M., Blythe, A.F., Snee, L.W., Copeland, P., Wright, J.E., Donelick, R.A., Guth, L.R., 2005. Overview of radiometric ages in three allochthonous belts of northern Venezuela: Old ones, new ones, and their impact on regional geology. In: Avé-Lallemant, H., Sisson, V., (eds.). Caribbean-South American Plate Interactions, Venezuela. Geological Society of America, 394 (Special Paper), 91-117.

Stacey, J.S., Kramers, J.D., 1975. Approximation of terrestrial lead isotope evolution by a twostage model. Earth and Planetary Science Letters, 26, 207-221.

Tassinari, C.C.G., Bettencourt, J.S., Geraldes, M.C., 2000. The Amazon craton. In: Cordani, U.G., Milani, E.J., Thomaz-Filho, A., Campos, D.A. (eds.). Tectonic evolution of South America. Rio de Janeiro, 31st International Geological Congress, 41-95.

Urbani, F., Wright, J., Grande, S., 2007. La Metadiorita de Todasana, Cordillera de la Costa, estado Vargas: Geología y geocronología. Caracas, Geos, 39, 93-94 and 33pp in CD.

Van Andel, T., 1958. Origin and classification of Cretaceous, Paleocene and Eocene sandstones of Western Venezuela. American Association of Petroleum Geologists Bulletin, 42, 734-763.

Viscarret, P., Wright, J.E., Urbani, F., 2007. Dataciones U/Pb SHRIMP en circón de rocas del macizo de El Baúl, estado Cojedes, Venezuela. Caracas, Geos, 39, 94-95 and 37pp in CD.

Villamil, T., Pindell, J.L., 1998. The Mesozoic of northern South America: foundations for sequence stratigraphic studies in passive margin strata deposited during non-glacial times. In: Pindell, J.L., Drake, C.L. (eds.). Paleogeographic Evolution and Non-glacial Eustasy, northern South America. Tulsa, Society for Sedimentary Geology (SEPM), 58 (Special Publications), 283-318.

Weber, B., Schaaf, P., Valencia, V.A., Iriondo, A., Ortega–Gutiérrez, F., 2006. Provenance ages of late Paleozoic sandstones (Santa Rosa Formation) from the Maya block, SE Mexico. Implications on the tectonic evolution of western Pangea. Revista Mexicana de Ciencias Geologicas, 23, 262-276.

Weber, B., Valencia, V.A., Schaaf, P., Pompa-Mera, V., Ruiz, J., 2008. Significance of provenance ages from the Chiapas Massif Complex (southeastern Mexico): Redefining the Paleozoic basement of the Maya block and its evolution in a Peri-Gondwanan realm. Journal of Geology, 116, 619-639.

Yoris, F., Ostos, M., Zamora, L., 1997. Petroleum Geology of Venezuela. In: Singer, J.M. (ed.). 1997 Venezuela Well Evaluation Conference. Schlumberger Surenco. Houston, Jolley Printing, 1-44.

Manuscript received November 2010;
revision accepted May 2011;
published Online June 2011.

ELECTRONIC APPENDIX

Sample Number	Unit	Longitude W	Latitude N
VMN-7	Aguardiente	70.109	10.1466
VMN-16	Bobare	69.448	10.4371
VMN-17	Bobare	69.4083	10.4024
VMN-18	Araure	69.097	9.6701
VMN-32	Barranquín	64.5351	10.2328
VMN-35	Barranquín	64.384	10.2919

Analysis	U (ppm)	^{206}Pb / ^{204}Pb	U/Th	$^{206}Pb^*$ / $^{207}Pb^*$	± (%)	Isotope ratios $^{207}Pb^*$ / $^{235}U^*$	± (%)	$^{206}Pb^*$ / ^{238}U	± (%)	error corr.	Apparent ages (Ma) $^{206}Pb^*$ / $^{238}U^*$	± (Ma)	$^{207}Pb^*$ / ^{235}U	± (Ma)	$^{206}Pb^*$ / $^{207}Pb^*$	± (Ma)	Best age (Ma)	± (Ma)
VMN7-1	66	4764	2.9	14.0971	1.9	1.5638	3.2	0.1599	2.5	0.80	956.1	22.6	956.0	19.7	955.6	39.3	956.1	22.6
VMN7-2	150	15084	2.5	10.5063	1.1	3.4787	1.5	0.2651	1.0	0.68	1515.8	13.5	1522.4	11.7	1531.6	20.6	1531.6	20.6
VMN7-3	370	14824	2.7	17.3221	1.3	0.6340	2.0	0.0796	1.5	0.76	494.0	7.3	498.6	8.0	519.5	29.1	494.0	7.3
VMN7-4	272	11912	4.3	16.6961	1.6	0.7951	2.5	0.0963	1.9	0.77	592.5	10.8	594.0	11.2	599.7	34.6	592.5	10.8
VMN7-5	277	25030	3.7	12.1967	1.5	2.2986	1.8	0.2033	1.0	0.56	1193.2	10.9	1211.9	12.7	1245.2	29.2	1245.2	29.2
VMN7-6	189	20970	1.3	10.3510	1.9	3.3996	2.1	0.2552	1.0	0.48	1465.3	13.5	1504.3	16.8	1559.6	35.1	1559.6	35.1
VMN7-7	207	26340	1.2	9.0124	1.4	4.7460	1.9	0.3102	1.3	0.67	1741.8	19.1	1775.4	15.7	1815.2	25.4	1815.2	25.4
VMN7-8	118	18190	1.7	8.9888	1.2	4.9720	2.0	0.3241	1.6	0.80	1809.9	24.9	1814.6	16.7	1819.9	21.4	1819.9	21.4
VMN7-9	66	7260	2.9	11.1524	1.3	2.9133	1.7	0.2356	1.0	0.60	1364.0	12.3	1385.4	12.7	1418.4	25.8	1418.4	25.8
VMN7-10	131	24314	1.3	7.6959	1.3	6.7098	1.6	0.3745	1.0	0.61	2050.6	17.6	2073.9	14.5	2097.1	22.8	2097.1	22.8
VMN7-11	523	44220	5.7	10.8854	1.1	2.9765	2.4	0.2350	2.1	0.89	1360.6	26.2	1401.6	18.2	1464.6	20.5	1464.6	20.5
VMN7-12	110	14620	2.1	9.0325	1.3	4.9843	1.9	0.3265	1.4	0.73	1821.5	21.9	1816.7	15.9	1811.1	23.3	1811.1	23.3
VMN7-13	126	13312	1.2	11.7191	1.3	2.6461	2.4	0.2249	2.1	0.85	1307.7	24.4	1313.6	17.9	1323.0	25.1	1323.0	25.1
VMN7-14	350	12628	1.8	16.6953	3.9	0.6585	8.5	0.0797	7.5	0.89	494.5	35.8	513.7	34.2	599.8	85.2	494.5	35.8
VMN7-15	76	8036	1.5	11.4783	1.4	2.7528	2.4	0.2292	1.9	0.80	1330.1	22.8	1342.9	17.7	1363.1	27.5	1363.1	27.5
VMN7-16	576	60090	2.7	9.3984	1.1	4.2008	2.5	0.2863	2.2	0.90	1623.2	32.0	1674.2	20.4	1738.6	20.3	1738.6	20.3
VMN7-17	270	28766	1.7	10.6598	1.0	3.2629	3.2	0.2523	3.0	0.95	1450.1	38.8	1472.3	24.5	1504.3	18.9	1504.3	18.9
VMN7-18	89	3436	0.9	17.9046	4.3	0.6438	4.5	0.0836	1.0	0.22	517.6	5.0	504.7	17.7	446.5	96.5	517.6	5.0
VMN7-19	166	14992	2.0	10.4255	1.7	3.6076	1.9	0.2728	1.0	0.52	1554.9	13.8	1551.2	15.4	1546.2	31.2	1546.2	31.2
VMN7-20	181	15116	2.3	11.2770	1.4	2.8485	2.3	0.2330	1.9	0.80	1350.1	22.7	1368.4	17.5	1397.2	26.7	1397.2	26.7
VMN7-21	227	5660	1.5	18.0454	3.0	0.5181	3.2	0.0678	1.0	0.33	423.0	4.3	423.9	11.0	429.0	67.0	423.0	4.3
VMN7-22	442	11662	3.8	17.5705	1.0	0.6334	3.3	0.0807	3.2	0.95	500.4	15.2	498.2	13.1	488.2	22.2	500.4	15.2
VMN7-23	322	8688	1.8	18.0769	1.0	0.5405	2.3	0.0709	2.1	0.89	441.3	8.7	438.7	8.2	425.1	22.8	441.3	8.7
VMN7-24	212	19058	3.2	12.4806	1.5	2.2619	2.1	0.2047	1.5	0.69	1200.7	16.1	1200.5	14.9	1200.0	30.0	1200.0	30.0
VMN7-25	108	11116	1.5	8.7304	1.0	5.3717	1.4	0.3401	1.0	0.71	1887.3	16.4	1880.3	12.1	1872.7	18.0	1872.7	18.0
VMN7-26	99	7878	2.6	13.8714	2.1	1.5869	2.3	0.1596	1.0	0.43	954.8	8.9	965.1	14.5	988.5	42.7	988.5	42.7
VMN7-27	162	14648	0.9	11.0021	1.7	2.4036	2.3	0.1918	1.5	0.65	1131.1	15.4	1243.7	16.4	1444.3	33.1	1444.3	33.1
VMN7-28	187	8750	1.8	17.7328	5.6	0.5934	5.8	0.0763	1.5	0.25	474.1	6.6	473.0	21.9	467.8	124.0	474.1	6.6
VMN7-30	50	7716	1.7	9.0622	1.6	4.8809	1.9	0.3208	1.0	0.52	1793.6	15.7	1799.0	16.2	1805.1	29.9	1805.1	29.9
VMN7-31	273	36986	3.6	10.2378	1.5	3.4655	2.2	0.2573	1.6	0.73	1476.1	20.8	1519.4	17.0	1580.2	27.3	1580.2	27.3
VMN7-32	680	80546	5.0	10.4007	1.1	3.4394	1.5	0.2594	1.0	0.69	1487.0	13.3	1513.4	11.5	1550.6	19.9	1550.6	19.9
VMN7-33	228	16602	3.5	13.6182	1.6	1.6794	1.9	0.1659	1.0	0.52	989.3	9.2	1000.8	12.1	1025.9	32.8	1025.9	32.8
VMN7-34	553	19184	5.7	15.2595	1.0	0.9616	2.5	0.1064	2.2	0.91	651.9	13.8	684.1	12.2	791.5	21.7	651.9	13.8
VMN7-35	181	11012	2.9	12.3779	1.6	2.0255	2.8	0.1818	2.3	0.82	1077.0	22.6	1124.1	18.9	1216.3	31.1	1216.3	31.1
VMN7-36	285	32606	2.7	9.4420	1.6	4.2635	2.5	0.2920	1.9	0.76	1651.3	27.1	1686.3	20.2	1730.1	29.4	1730.1	29.4
VMN7-37	259	18022	2.7	13.4915	1.4	1.7730	1.7	0.1735	1.0	0.59	1031.3	9.5	1035.6	10.9	1044.7	27.3	1044.7	27.3
VMN7-38	150	4874	2.1	18.4810	4.1	0.5129	4.4	0.0687	1.6	0.35	428.6	6.4	420.4	15.2	375.6	92.9	428.6	6.4
VMN7-39	49	4636	1.5	11.1848	1.7	2.8587	2.4	0.2319	1.6	0.69	1344.4	19.9	1371.1	17.9	1412.9	33.1	1412.9	33.1
VMN7-40	107	10662	5.7	12.1272	1.4	2.4690	1.7	0.2172	1.0	0.59	1266.8	11.5	1263.0	12.3	1256.4	26.8	1256.4	26.8
VMN7-41	268	29192	3.1	9.0964	1.3	4.7650	2.2	0.3144	1.8	0.82	1762.1	27.8	1778.7	18.4	1798.3	22.9	1798.3	22.9
VMN7-42	217	24674	1.9	9.0510	1.1	4.8895	1.5	0.3210	1.0	0.69	1794.4	15.7	1800.4	12.3	1807.4	19.3	1807.4	19.3
VMN7-43	235	23662	2.3	9.5679	1.3	3.9897	1.7	0.2769	1.0	0.60	1575.5	14.0	1632.1	13.4	1705.8	24.3	1705.8	24.3
VMN7-44	75	3304	2.6	13.1479	3.8	1.8502	4.0	0.1764	1.0	0.26	1047.5	10.1	1063.5	26.1	1096.6	76.5	1096.6	76.5
VMN7-45	260	4476	1.4	5.3367	1.5	12.1056	1.8	0.4685	1.0	0.56	2477.2	20.6	2612.6	16.9	2719.3	24.6	2719.3	24.6
VMN7-46	252	10330	5.2	15.9285	2.4	0.8440	2.6	0.0975	1.0	0.39	599.7	5.7	621.3	12.1	700.8	51.0	599.7	5.7

DOI: 10.1344/105.000001698

Analysis	U (ppm)	^{206}Pb ^{204}Pb	U/Th	$^{206}Pb^*$ $^{207}Pb^*$	± (%)	Isotope ratios $^{207}Pb^*$ $^{235}U^*$	± (%)	$^{206}Pb^*$ ^{238}U	± (%)	error corr.	Apparent ages (Ma) $^{206}Pb^*$ $^{238}U^*$	± (Ma)	$^{207}Pb^*$ ^{235}U	± (Ma)	$^{206}Pb^*$ $^{207}Pb^*$	± (Ma)	Best age (Ma)	± (Ma)
VMN7-47	154	14614	2.6	10.9279	1.6	3.2214	1.9	0.2553	1.0	0.53	1465.9	13.1	1462.3	14.7	1457.2	30.5	1457.2	30.5
VMN7-48	465	30088	16.7	12.6979	1.6	2.0820	1.9	0.1917	1.0	0.53	1130.8	10.4	1142.9	12.9	1165.9	31.7	1165.9	31.7
VMN7-49	105	9874	1.9	11.2009	2.2	3.0753	2.6	0.2498	1.4	0.53	1437.6	17.7	1426.5	19.8	1410.1	41.9	1410.1	41.9
VMN7-50	195	23450	2.7	10.8089	1.4	3.3093	1.7	0.2594	1.0	0.59	1486.9	13.3	1483.2	13.1	1478.0	25.6	1478.0	25.6
VMN7-51	191	2322	0.4	9.1721	6.8	4.0125	7.3	0.2669	2.8	0.38	1525.2	38.0	1636.7	59.7	1783.2	123.7	1783.2	123.7
VMN7-52	60	4732	1.6	12.6407	1.9	2.2285	2.2	0.2043	1.0	0.46	1198.4	10.9	1190.0	15.2	1174.9	38.1	1174.9	38.1
VMN7-54	60	6504	1.6	10.9445	1.1	3.2314	1.5	0.2565	1.0	0.67	1471.9	13.2	1464.7	11.6	1454.3	21.3	1454.3	21.3
VMN7-55	138	6582	2.1	10.9826	3.1	3.1980	3.2	0.2547	1.0	0.31	1462.8	13.1	1456.7	25.0	1447.7	58.4	1447.7	58.4
VMN7-57	298	19026	3.2	8.8660	1.1	4.5403	4.8	0.2920	4.7	0.97	1651.3	68.2	1738.4	40.1	1844.8	20.3	1844.8	20.3
VMN7-58	158	15400	2.5	10.0679	2.3	3.7593	2.5	0.2745	1.0	0.39	1563.6	13.9	1584.1	20.4	1611.5	43.7	1611.5	43.7
VMN7-59	122	19108	1.4	8.6147	1.5	5.5143	1.8	0.3445	1.0	0.54	1908.4	16.5	1902.8	15.8	1896.7	27.7	1896.7	27.7
VMN7-60	175	25064	1.5	9.3360	1.0	4.4268	1.4	0.2997	1.0	0.71	1690.0	14.9	1717.4	11.7	1750.8	18.3	1750.8	18.3
VMN7-61	257	25656	4.1	12.2281	1.5	2.4207	2.0	0.2147	1.4	0.66	1253.7	15.4	1248.8	14.6	1240.2	29.8	1240.2	29.8
VMN7-62	187	32398	3.2	9.0226	1.8	5.0578	2.0	0.3310	1.0	0.50	1843.1	16.0	1829.1	17.1	1813.1	31.8	1813.1	31.8
VMN7-63	328	31360	4.0	12.4118	1.0	2.3180	1.9	0.2087	1.7	0.86	1221.7	18.6	1217.8	13.8	1210.9	19.8	1210.9	19.8
VMN7-64	291	14360	1.7	8.7138	2.9	3.7649	6.1	0.2379	5.4	0.88	1376.0	66.3	1585.3	48.8	1876.1	52.0	1876.1	52.0
VMN7-65	29	3146	2.3	11.1436	3.0	3.1483	3.2	0.2545	1.0	0.31	1461.4	13.1	1444.6	24.7	1419.9	58.3	1419.9	58.3
VMN7-66	180	19970	1.6	9.0436	1.0	4.9239	1.4	0.3230	1.0	0.71	1804.2	15.7	1806.4	11.9	1808.9	18.2	1808.9	18.2
VMN7-67	60	5000	2.1	13.6733	2.0	1.7237	2.2	0.1709	1.0	0.45	1017.3	9.4	1017.4	14.2	1017.7	39.7	1017.7	39.7
VMN7-68	27	3274	0.7	10.4124	2.1	3.6314	2.4	0.2742	1.2	0.49	1562.3	16.1	1556.4	18.8	1548.5	38.6	1548.5	38.6
VMN7-69	148	17956	2.0	9.5061	2.5	3.6897	4.7	0.2544	4.0	0.85	1461.0	52.6	1569.1	37.8	1717.7	45.8	1717.7	45.8
VMN7-70	305	9260	1.8	17.1814	1.3	0.6909	2.1	0.0861	1.7	0.79	532.4	8.5	533.3	8.8	537.4	28.8	532.4	8.5
VMN7-71	108	11984	4.0	10.6289	1.3	3.3963	1.6	0.2618	1.0	0.61	1499.1	13.4	1503.5	12.8	1509.8	24.4	1509.8	24.4
VMN7-72	502	13322	2.7	18.2059	1.4	0.5037	1.7	0.0665	1.0	0.59	415.1	4.1	414.2	5.8	409.2	30.7	415.1	4.1
VMN7-73	168	13830	3.4	12.9019	1.9	1.9891	2.6	0.1861	1.8	0.68	1100.4	17.9	1111.8	17.7	1134.3	38.4	1134.3	38.4
VMN7-74	360	41838	3.1	9.8368	1.3	4.1145	3.8	0.2935	3.6	0.94	1659.2	51.9	1657.2	30.8	1654.6	23.4	1654.6	23.4
VMN7-75	88	12158	2.3	11.3293	2.1	3.0177	2.5	0.2480	1.4	0.55	1427.9	17.7	1412.1	19.2	1388.3	40.6	1388.3	40.6
VMN7-76	57	8176	1.3	10.1719	1.0	3.7919	1.4	0.2797	1.0	0.71	1590.1	14.1	1591.0	11.4	1592.3	18.8	1592.3	18.8
VMN7-77	76	5434	1.2	14.9917	2.7	1.2972	2.9	0.1410	1.0	0.35	850.6	8.0	844.5	16.6	828.5	56.7	850.6	8.0
VMN7-78	352	57368	6.4	8.4232	1.3	5.7625	1.6	0.3520	1.0	0.62	1944.3	16.8	1940.8	14.1	1937.0	22.9	1937.0	22.9
VMN7-79	72	11060	1.4	9.4395	1.3	4.4842	1.6	0.3070	1.0	0.61	1725.9	15.1	1728.0	13.6	1730.6	23.9	1730.6	23.9
VMN7-80	218	20446	3.3	12.1205	1.0	2.4329	1.4	0.2139	1.0	0.71	1249.4	11.4	1252.4	10.2	1257.5	19.6	1257.5	19.6
VMN7-81	167	7852	2.2	16.5881	1.9	0.8300	2.6	0.0999	1.8	0.68	613.6	10.2	613.6	11.9	613.8	40.8	613.6	10.2
VMN7-82	211	28214	2.3	11.2215	1.5	2.9324	2.1	0.2387	1.5	0.72	1379.7	18.8	1390.3	15.9	1406.6	27.8	1406.6	27.8
VMN7-83	118	15510	1.2	9.4434	1.0	4.5451	1.8	0.3113	1.5	0.83	1747.1	22.6	1739.3	14.9	1729.9	18.4	1729.9	18.4
VMN7-84	279	10600	3.1	17.5872	1.0	0.6409	1.7	0.0818	1.3	0.80	506.6	6.5	502.9	6.7	486.1	22.3	506.6	6.5
VMN7-86	114	7818	1.8	8.6526	1.0	5.4525	2.2	0.3422	2.0	0.89	1897.1	32.2	1893.1	19.0	1888.8	18.4	1888.8	18.4
VMN7-87	174	9834	2.7	11.0736	1.0	3.0611	1.4	0.2458	1.0	0.69	1417.0	12.7	1423.0	11.1	1432.0	19.9	1432.0	19.9
VMN7-88	439	32810	3.6	12.1402	1.2	2.4680	1.5	0.2173	1.0	0.66	1267.6	11.5	1262.7	11.0	1254.3	22.5	1254.3	22.5
VMN7-89	391	13794	2.3	16.4681	1.9	0.8962	2.2	0.1070	1.0	0.46	655.5	6.2	649.7	10.4	629.4	41.4	655.5	6.2
VMN7-90	79	4328	1.8	13.8176	2.1	1.7006	2.3	0.1704	1.1	0.46	1014.5	9.9	1008.8	14.8	996.4	41.8	996.4	41.8
VMN7-91	173	21374	2.8	11.1451	1.0	2.9178	1.4	0.2358	1.0	0.70	1365.1	12.3	1386.5	10.8	1419.7	19.5	1419.7	19.5
VMN7-92	200	20584	2.2	9.0117	1.2	4.8262	2.4	0.3154	2.1	0.86	1767.4	31.7	1789.5	20.2	1815.3	22.5	1815.3	22.5
VMN7-93	50	4734	1.6	12.2103	2.1	2.4334	2.3	0.2155	1.0	0.44	1258.0	11.4	1252.5	16.5	1243.1	40.3	1243.1	40.3
VMN7-94	59	5898	3.7	12.7241	2.5	2.0662	2.8	0.1907	1.2	0.42	1125.0	12.1	1137.7	19.1	1161.8	50.3	1161.8	50.3

DOI: 10.1344/105.000001698

Analysis	U (ppm)	^{206}Pb / ^{204}Pb	U/Th	$^{206}Pb^*$ / $^{207}Pb^*$	± (%)	Isotope ratios $^{207}Pb^*$ / $^{235}U^*$	± (%)	$^{206}Pb^*$ / ^{238}U	± (%)	error corr.	Apparent ages (Ma) $^{206}Pb^*$ / $^{238}U^*$	± (Ma)	$^{207}Pb^*$ / ^{235}U	± (Ma)	$^{206}Pb^*$ / $^{207}Pb^*$	± (Ma)	Best age (Ma)	± (Ma)
VMN7-95	200	16444	4.7	13.8750	1.3	1.5545	1.6	0.1564	1.0	0.62	936.9	8.7	952.3	10.0	988.0	25.9	936.9	8.7
VMN7-96	249	19972	4.8	9.0103	1.0	4.4705	1.4	0.2921	1.0	0.71	1652.2	14.6	1725.5	11.7	1815.6	18.2	1815.6	18.2
VMN7-97	260	26020	1.9	7.5682	1.0	6.0310	1.4	0.3310	1.0	0.70	1843.4	16.0	1980.3	12.4	2126.5	17.9	2126.5	17.9
VMN7-98	142	14778	4.0	13.0275	1.0	1.9202	1.4	0.1814	1.0	0.70	1074.8	9.9	1088.2	9.5	1115.0	20.1	1115.0	20.1
VMN7-99	149	14188	2.6	10.9750	1.0	2.9202	1.9	0.2324	1.6	0.85	1347.3	19.9	1387.2	14.5	1449.0	19.1	1449.0	19.1
VMN7-100	420	46768	2.9	10.2054	1.1	3.4354	3.6	0.2543	3.4	0.95	1460.5	44.7	1512.5	28.2	1586.2	20.0	1586.2	20.0
VMN16-1	212	22328	3.1	13.0226	1.8	1.9354	2.0	0.1828	1.0	0.50	1082.2	10.0	1093.4	13.5	1115.7	34.9	1115.7	34.9
VMN16-2	120	11214	2.2	13.8972	1.7	1.5803	2.0	0.1593	1.1	0.52	952.8	9.3	962.5	12.7	984.7	35.5	952.8	9.3
VMN16-3	100	9836	3.1	14.1958	1.3	1.5741	1.8	0.1621	1.2	0.67	968.3	10.8	960.1	11.1	941.3	27.1	968.3	10.8
VMN16-4	256	22858	1.9	9.7466	1.0	3.3663	5.6	0.2380	5.5	0.98	1376.1	67.9	1496.6	43.6	1671.7	18.5	1671.7	18.5
VMN16-5	185	14056	1.2	14.3542	1.0	1.4351	1.4	0.1494	1.0	0.71	897.6	8.4	903.7	8.5	918.5	20.6	897.6	8.4
VMN16-6	54	4762	2.2	14.3276	1.5	1.5027	1.8	0.1561	1.0	0.55	935.3	8.7	931.5	11.1	922.3	31.1	935.3	8.7
VMN16-7	105	9022	2.3	14.1570	1.4	1.4769	1.7	0.1516	1.0	0.58	910.2	8.5	921.0	10.4	946.9	28.5	910.2	8.5
VMN16-8	176	21734	1.5	10.4973	1.1	3.3317	1.5	0.2537	1.0	0.69	1457.3	13.0	1488.5	11.3	1533.3	19.8	1533.3	19.8
VMN16-9	144	13404	1.8	13.9292	2.1	1.5510	2.3	0.1567	1.0	0.44	938.4	8.7	950.9	14.1	980.0	41.9	938.4	8.7
VMN16-10	668	33500	1.8	10.5920	1.9	2.4416	3.2	0.1876	2.6	0.80	1108.2	26.0	1254.9	23.0	1516.3	36.2	1516.3	36.2
VMN16-11	220	18502	2.5	13.7947	1.8	1.6176	2.1	0.1618	1.0	0.48	967.0	9.0	977.0	13.0	999.8	36.8	999.8	36.8
VMN16-12	171	14464	4.2	13.7377	1.6	1.6810	1.9	0.1675	1.0	0.53	998.2	9.2	1001.4	12.0	1008.2	32.6	1008.2	32.6
VMN16-13	106	10458	2.4	14.0828	1.7	1.5335	2.0	0.1566	1.0	0.50	938.0	8.7	943.9	12.3	957.6	35.4	938.0	8.7
VMN16-14	130	12136	2.7	13.8778	1.5	1.6007	1.8	0.1611	1.0	0.56	963.0	8.9	970.5	11.2	987.5	30.3	987.5	30.3
VMN16-16	116	13992	1.8	11.0896	1.6	3.0780	1.9	0.2476	1.0	0.53	1425.9	12.8	1427.2	14.4	1429.2	30.4	1429.2	30.4
VMN16-17	147	12812	3.9	14.0921	1.1	1.5738	1.5	0.1608	1.0	0.68	961.5	9.3	959.9	9.5	956.3	23.0	961.5	9.3
VMN16-18	148	25412	1.5	9.0216	1.1	4.8612	1.5	0.3181	1.0	0.66	1780.3	15.6	1795.6	12.7	1813.3	20.5	1813.3	20.5
VMN16-19	82	14772	1.6	9.2266	1.4	4.6623	1.7	0.3120	1.0	0.58	1750.5	15.3	1760.5	14.4	1772.4	25.6	1772.4	25.6
VMN16-20	354	27674	3.2	12.6796	2.2	1.8306	3.1	0.1683	2.2	0.70	1003.0	20.4	1056.5	20.5	1168.8	44.0	1168.8	44.0
VMN16-21	182	19212	2.5	12.6124	1.8	2.1831	2.0	0.1997	1.0	0.49	1173.7	10.7	1175.7	14.2	1179.3	35.2	1179.3	35.2
VMN16-22	130	11852	1.2	13.7905	1.9	1.6616	2.2	0.1662	1.2	0.53	991.1	10.7	994.0	14.0	1000.4	38.0	1000.4	38.0
VMN16-23	106	17714	1.8	9.0263	1.0	4.9341	1.4	0.3230	1.0	0.71	1804.4	15.7	1808.1	11.9	1812.4	18.2	1812.4	18.2
VMN16-24	114	21160	2.3	9.1060	2.1	4.8017	2.3	0.3171	1.0	0.44	1775.7	15.5	1785.2	19.2	1796.4	37.3	1796.4	37.3
VMN16-25	50	7778	1.9	10.0103	1.7	3.8515	2.1	0.2796	1.2	0.57	1589.5	17.2	1603.6	17.1	1622.2	32.4	1622.2	32.4
VMN16-26	146	10216	2.9	13.7906	2.8	1.5596	3.4	0.1560	2.0	0.58	934.5	17.3	954.3	21.2	1000.4	56.5	934.5	17.3
VMN16-28	241	4536	1.9	11.3894	4.0	2.2737	7.9	0.1878	6.8	0.86	1109.6	69.0	1204.2	55.6	1378.1	77.2	1378.1	77.2
VMN16-29	371	41946	1.8	10.7799	4.3	2.7221	6.1	0.2128	4.4	0.72	1243.8	49.5	1334.5	45.5	1483.1	81.0	1483.1	81.0
VMN16-30	166	19552	1.5	12.2305	1.5	2.2232	2.1	0.1972	1.4	0.68	1160.3	15.1	1188.4	14.5	1239.8	29.7	1239.8	29.7
VMN16-31	175	15658	3.1	13.6246	1.6	1.6749	1.9	0.1655	1.0	0.53	987.3	9.2	999.1	11.9	1024.9	32.0	1024.9	32.0
VMN16-32	191	17966	3.6	13.5344	1.6	1.6608	2.2	0.1630	1.5	0.69	973.6	13.7	993.7	13.9	1038.3	32.0	1038.3	32.0
VMN16-33	85	13366	1.3	9.0361	1.4	4.7638	1.7	0.3122	1.0	0.59	1751.5	15.3	1778.5	14.2	1810.4	24.7	1810.4	24.7
VMN16-34	154	11062	0.7	8.5901	1.0	5.1933	1.6	0.3236	1.3	0.79	1807.0	20.2	1851.5	13.9	1901.8	18.1	1901.8	18.1
VMN16-35	42	2046	1.6	17.2447	6.2	0.7730	6.3	0.0967	1.1	0.17	594.9	6.1	581.5	27.9	529.3	135.9	594.9	6.1
VMN16-36	190	25318	1.6	10.0772	1.0	3.8798	1.4	0.2836	1.0	0.71	1609.3	14.2	1609.5	11.4	1609.8	18.6	1609.8	18.6
VMN16-37	235	12042	3.9	13.0309	1.8	1.7821	2.0	0.1684	1.0	0.49	1003.4	9.3	1039.0	13.3	1114.4	35.7	1114.4	35.7
VMN16-38	78	6850	3.4	13.8067	3.0	1.7509	3.2	0.1753	1.0	0.31	1041.4	9.6	1027.5	20.6	998.0	61.4	998.0	61.4
VMN16-39	325	14404	3.6	13.6340	1.0	1.6141	1.4	0.1596	1.0	0.71	954.6	8.9	975.7	8.9	1023.5	20.3	1023.5	20.3
VMN16-40	195	18390	3.2	13.5666	2.2	1.7280	2.4	0.1700	1.0	0.42	1012.3	9.4	1019.0	15.4	1033.5	44.1	1033.5	44.1
VMN16-41	90	8440	1.4	12.9217	1.4	2.0100	2.3	0.1884	1.9	0.81	1112.5	19.3	1118.9	15.8	1131.2	27.3	1131.2	27.3

DOI: 10.1344/105.000001698

Analysis	U (ppm)	$^{206}Pb/^{204}Pb$	U/Th	$^{206}Pb^*/^{207}Pb^*$	± (%)	Isotope ratios $^{207}Pb^*/^{235}U^*$	± (%)	$^{206}Pb^*/^{238}U$	± (%)	error corr.	Apparent ages (Ma) $^{206}Pb^*/^{238}U^*$	± (Ma)	$^{207}Pb^*/^{235}U$	± (Ma)	$^{206}Pb^*/^{207}Pb^*$	± (Ma)	Best age (Ma)	± (Ma)
VMN16-43	136	6512	1.5	13.6139	2.5	1.6645	3.9	0.1643	3.0	0.77	980.9	27.4	995.1	24.8	1026.5	50.5	1026.5	50.5
VMN16-44	200	10452	2.7	16.1816	1.3	0.9040	2.1	0.1061	1.6	0.78	650.0	10.1	653.9	10.1	667.1	28.4	650.0	10.1
VMN16-45	170	19896	1.1	10.4805	1.4	3.4286	3.1	0.2606	2.7	0.89	1493.0	36.5	1511.0	24.1	1536.3	25.8	1536.3	25.8
VMN16-46	166	13598	3.2	14.0613	3.8	1.5982	3.9	0.1630	1.0	0.25	973.4	9.0	969.5	24.6	960.8	78.0	973.4	9.0
VMN16-47	64	12402	1.3	9.2582	2.9	4.4409	3.1	0.2982	1.0	0.33	1682.3	14.8	1720.0	25.4	1766.1	53.0	1766.1	53.0
VMN16-48	359	33106	6.0	13.6003	1.3	1.6506	1.7	0.1628	1.0	0.60	972.4	9.0	989.8	10.5	1028.5	26.9	1028.5	26.9
VMN16-49	83	8136	3.0	14.2147	3.0	1.4759	3.1	0.1522	1.0	0.32	913.0	8.5	920.5	19.0	938.6	61.1	913.0	8.5
VMN16-50	71	6994	6.9	13.9116	2.9	1.4520	3.3	0.1465	1.5	0.45	881.3	12.3	910.7	19.9	982.6	60.1	881.3	12.3
VMN16-51	90	14824	2.8	10.7303	2.6	2.9477	2.8	0.2294	1.0	0.35	1331.3	12.0	1394.2	21.4	1491.8	50.0	1491.8	50.0
VMN16-52	100	10706	3.5	14.2681	1.9	1.5591	2.1	0.1613	1.0	0.47	964.2	9.0	954.1	13.3	930.9	39.0	964.2	9.0
VMN16-53	464	72538	5.8	10.4828	1.0	3.5232	1.4	0.2679	1.0	0.69	1529.9	13.6	1532.4	11.4	1535.9	19.6	1535.9	19.6
VMN16-54	84	11638	4.5	11.3254	2.3	2.8717	2.7	0.2359	1.6	0.57	1365.3	19.3	1374.5	20.7	1388.9	43.3	1388.9	43.3
VMN16-55	228	21696	2.2	14.3340	2.9	1.4344	3.1	0.1491	1.0	0.32	896.0	8.4	903.4	18.4	921.4	59.9	896.0	8.4
VMN16-56	110	11326	1.3	12.7392	1.3	2.1230	1.6	0.1961	1.0	0.62	1154.6	10.6	1156.3	11.1	1159.5	25.0	1159.5	25.0
VMN16-57	208	15828	3.0	14.0108	1.3	1.5853	1.7	0.1611	1.2	0.69	962.9	10.6	964.5	10.7	968.1	25.5	962.9	10.6
VMN16-58	93	9552	2.9	12.4737	1.3	2.2500	1.6	0.2036	1.0	0.61	1194.4	10.9	1196.8	11.4	1201.1	25.3	1201.1	25.3
VMN16-60	109	15716	1.8	8.6538	1.3	5.0338	1.9	0.3159	1.4	0.73	1769.9	22.1	1825.0	16.5	1888.6	23.8	1888.6	23.8
VMN16-61	113	9946	2.1	13.4479	2.5	1.7289	2.7	0.1686	1.0	0.37	1004.5	9.3	1019.3	17.6	1051.3	51.3	1051.3	51.3
VMN16-62	263	14096	0.5	16.5708	1.8	0.8626	2.1	0.1037	1.0	0.48	635.9	6.1	631.5	9.8	616.0	39.6	635.9	6.1
VMN16-63	33	3816	0.6	10.5936	2.2	3.4707	2.5	0.2667	1.0	0.41	1523.8	13.6	1520.6	19.4	1516.0	42.3	1516.0	42.3
VMN16-64	148	11832	3.1	13.5025	1.5	1.7455	1.8	0.1709	1.0	0.55	1017.3	9.4	1025.5	11.8	1043.1	30.9	1043.1	30.9
VMN16-65	200	18810	1.8	13.7987	2.5	1.6675	2.7	0.1669	1.0	0.38	994.9	9.2	996.2	16.9	999.2	50.2	999.2	50.2
VMN16-66	66	5554	2.2	14.3248	2.5	1.5431	2.7	0.1603	1.0	0.37	958.5	8.9	947.7	16.9	922.7	52.3	958.5	8.9
VMN16-67	324	10184	1.6	17.6593	2.1	0.5664	2.3	0.0725	1.0	0.44	451.4	4.4	455.7	8.4	477.0	45.8	451.4	4.4
VMN16-68	171	14620	2.7	13.7893	1.7	1.6004	2.1	0.1601	1.2	0.60	957.1	11.0	970.4	13.0	1000.6	33.8	1000.6	33.8
VMN16-69	193	14112	3.0	14.3549	1.8	1.4289	2.0	0.1488	1.0	0.50	894.0	8.3	901.1	12.1	918.4	36.0	894.0	8.3
VMN16-70	144	12202	2.6	12.8701	1.3	2.0077	2.1	0.1874	1.6	0.77	1107.3	16.2	1118.1	13.9	1139.2	25.9	1139.2	25.9
VMN16-71	174	21176	3.4	10.7619	1.0	3.3596	1.4	0.2622	1.0	0.71	1501.2	13.4	1495.0	11.1	1486.3	19.0	1486.3	19.0
VMN16-72	284	26438	2.6	13.0644	2.1	1.9449	2.3	0.1843	1.0	0.44	1090.3	10.0	1096.7	15.4	1109.3	41.2	1109.3	41.2
VMN16-73	94	10706	1.9	11.7139	1.3	2.7025	1.7	0.2296	1.0	0.60	1332.4	12.0	1329.1	12.4	1323.9	26.1	1323.9	26.1
VMN16-74	42	3832	2.2	14.0321	3.3	1.5881	3.8	0.1616	1.9	0.49	965.8	16.6	965.6	23.6	965.0	67.7	965.8	16.6
VMN16-75	229	29694	2.2	10.2545	1.0	3.6845	2.6	0.2740	2.4	0.92	1561.2	32.6	1568.0	20.4	1577.2	18.7	1577.2	18.7
VMN16-76	122	13544	4.5	13.7312	1.4	1.6768	2.0	0.1670	1.4	0.72	995.5	13.1	999.8	12.6	1009.1	28.0	1009.1	28.0
VMN16-77	117	11058	3.3	13.5871	1.4	1.7469	1.8	0.1721	1.2	0.65	1023.9	11.0	1026.0	11.6	1030.5	27.6	1030.5	27.6
VMN16-78	123	14506	2.3	10.3286	1.4	2.9501	9.1	0.2210	9.0	0.99	1287.1	104.4	1394.9	68.8	1563.7	25.5	1563.7	25.5
VMN16-79	270	11432	1.9	12.3908	1.3	2.2649	1.7	0.2035	1.2	0.67	1194.3	12.6	1201.4	12.2	1214.3	25.5	1214.3	25.5
VMN16-80	746	53290	2.1	14.2053	1.4	1.4956	1.7	0.1541	1.0	0.60	923.8	8.6	928.6	10.2	939.9	27.7	923.8	8.6
VMN16-81	295	19580	2.9	13.5058	1.7	1.7990	2.0	0.1762	1.0	0.50	1046.3	9.7	1045.1	13.1	1042.6	35.2	1042.6	35.2
VMN16-82	67	8592	1.4	8.1085	1.0	6.0310	2.2	0.3547	2.0	0.89	1956.9	33.4	1980.3	19.3	2004.9	17.8	2004.9	17.8
VMN16-83	117	15106	1.6	9.0038	1.3	4.5725	1.8	0.2986	1.2	0.67	1684.3	17.3	1744.3	14.6	1816.9	23.8	1816.9	23.8
VMN16-84	181	10292	2.6	13.2436	4.5	1.7151	4.6	0.1647	1.3	0.28	983.1	11.9	1014.2	29.8	1082.0	89.3	1082.0	89.3
VMN16-85	268	20774	3.5	12.2173	1.5	2.2560	5.2	0.1999	5.0	0.96	1174.8	53.3	1198.7	36.4	1241.9	28.4	1241.9	28.4
VMN17-1	130	20484	2.1	8.9249	1.3	4.4875	2.3	0.2905	1.8	0.82	1643.9	26.7	1728.7	18.7	1832.8	23.6	1832.8	23.6
VMN17-2	80	10618	2.5	11.3360	1.2	2.6819	3.0	0.2205	2.7	0.91	1284.5	31.9	1323.5	22.2	1387.1	23.7	1387.1	23.7
VMN17-3	38	3244	2.7	14.7601	3.2	1.3761	4.6	0.1473	3.4	0.73	885.9	27.7	878.8	27.2	860.9	65.9	885.9	27.7

DOI: 10.1344/105.000001698

Analysis	U (ppm)	^{206}Pb / ^{204}Pb	U/Th	$^{206}Pb^*$ / $^{207}Pb^*$	± (%)	Isotope ratios $^{207}Pb^*$ / $^{235}U^*$	± (%)	$^{206}Pb^*$ / ^{238}U	± (%)	error corr.	Apparent ages (Ma) $^{206}Pb^*$ / $^{238}U^*$	± (Ma)	$^{207}Pb^*$ / ^{235}U	± (Ma)	$^{206}Pb^*$ / $^{207}Pb^*$	± (Ma)	Best age (Ma)	± (Ma)
VMN17-4	274	24778	3.0	12.3387	1.6	2.1186	2.5	0.1896	1.9	0.77	1119.2	19.9	1154.9	17.4	1222.5	31.7	1222.5	31.7
VMN17-5	142	17762	2.4	10.8512	2.0	3.1165	2.3	0.2453	1.0	0.44	1414.0	12.7	1436.8	17.5	1470.6	38.7	1470.6	38.7
VMN17-6	77	5846	2.4	14.0587	3.6	1.5831	3.7	0.1614	1.0	0.27	964.7	9.0	963.6	23.2	961.1	73.5	964.7	9.0
VMN17-7	44	3608	2.2	14.2737	4.0	1.5156	4.1	0.1569	1.0	0.24	939.5	8.7	936.7	25.2	930.1	82.1	939.5	8.7
VMN17-8	97	14750	1.4	9.0818	1.1	4.6520	3.8	0.3064	3.6	0.96	1723.0	54.6	1758.7	31.5	1801.2	19.7	1801.2	19.7
VMN17-9	272	14818	10.0	14.8904	1.8	0.9252	5.1	0.0999	4.8	0.94	613.9	28.2	665.1	25.1	842.6	38.0	613.9	28.2
VMN17-10	166	12654	1.3	14.1391	1.7	1.5645	3.5	0.1604	3.0	0.87	959.2	27.1	956.3	21.7	949.5	35.5	959.2	27.1
VMN17-11	166	18426	3.1	11.5998	1.7	2.4368	2.0	0.2050	1.0	0.50	1202.2	11.0	1253.5	14.3	1342.8	33.3	1342.8	33.3
VMN17-12	184	16782	0.8	13.6160	1.4	1.5955	2.3	0.1576	1.8	0.78	943.2	15.5	968.4	14.2	1026.2	29.0	1026.2	29.0
VMN17-13	82	7650	1.4	14.2498	2.1	1.4866	2.3	0.1536	1.0	0.43	921.3	8.6	924.9	14.2	933.5	43.5	921.3	8.6
VMN17-14	96	9514	2.2	13.6516	1.7	1.6911	2.0	0.1674	1.0	0.51	998.0	9.2	1005.2	12.5	1020.9	33.9	1020.9	33.9
VMN17-15	193	18072	2.9	12.5151	1.3	1.9433	1.9	0.1764	1.4	0.73	1047.2	13.4	1096.1	12.7	1194.6	25.5	1194.6	25.5
VMN17-16	68	5276	1.1	14.1047	2.2	1.5647	3.7	0.1601	3.0	0.81	957.1	26.9	956.3	23.0	954.5	44.2	957.1	26.9
VMN17-17	141	13228	2.5	13.8334	1.2	1.6065	2.1	0.1612	1.7	0.81	963.3	15.1	972.7	13.0	994.1	24.5	994.1	24.5
VMN17-18	46	3518	3.9	14.1313	2.9	1.5025	3.1	0.1540	1.0	0.33	923.3	8.6	931.4	18.6	950.6	59.1	923.3	8.6
VMN17-19	519	63186	2.6	10.5330	1.0	3.4345	1.6	0.2624	1.2	0.77	1501.9	16.1	1512.3	12.3	1526.9	18.8	1526.9	18.8
VMN17-20	85	7374	3.0	12.6042	1.4	2.1399	2.8	0.1956	2.4	0.86	1151.7	25.3	1161.8	19.3	1180.6	27.9	1180.6	27.9
VMN17-21	48	8120	1.7	8.9747	1.9	4.8513	2.2	0.3158	1.2	0.52	1769.1	17.8	1793.8	18.7	1822.8	34.4	1822.8	34.4
VMN17-22	38	3282	1.9	14.2944	3.8	1.5713	3.9	0.1629	1.0	0.26	972.9	9.1	959.0	24.2	927.1	77.3	972.9	9.1
VMN17-23	83	7538	2.0	13.9847	1.9	1.6074	2.2	0.1630	1.2	0.53	973.6	10.6	973.1	13.9	971.9	38.3	971.9	38.3
VMN17-24	53	4938	2.6	13.7654	2.9	1.6729	3.1	0.1670	1.0	0.32	995.7	9.2	998.3	19.8	1004.1	59.8	1004.1	59.8
VMN17-25	64	8192	1.5	11.8474	1.9	2.5610	2.2	0.2201	1.0	0.48	1282.2	12.1	1289.6	16.0	1301.9	37.3	1301.9	37.3
VMN17-26	54	4550	2.8	14.6758	3.0	1.4323	4.4	0.1525	3.2	0.73	914.7	27.4	902.5	26.1	872.8	61.5	914.7	27.4
VMN17-27	179	15490	2.4	13.6640	1.1	1.6590	2.6	0.1644	2.3	0.90	981.2	21.0	993.0	16.3	1019.1	22.8	1019.1	22.8
VMN17-28	67	6900	1.6	13.7884	1.7	1.6832	3.7	0.1683	3.3	0.89	1002.9	30.5	1002.2	23.4	1000.7	33.6	1000.7	33.6
VMN17-29	239	20716	4.8	13.7242	1.4	1.6578	2.3	0.1650	1.8	0.80	984.6	16.6	992.5	14.5	1010.2	28.0	1010.2	28.0
VMN17-30	84	6834	3.4	13.7796	1.8	1.5065	3.1	0.1506	2.5	0.80	904.1	21.0	933.0	18.9	1002.0	37.4	904.1	21.0
VMN17-31	46	4450	3.1	13.5818	2.8	1.8148	3.0	0.1788	1.0	0.33	1060.2	9.8	1050.8	19.6	1031.3	57.1	1031.3	57.1
VMN17-32	46	4030	1.7	14.0503	3.7	1.5480	3.8	0.1577	1.0	0.26	944.2	8.9	949.7	23.6	962.4	75.2	944.2	8.9
VMN17-33	49	4964	2.8	13.7219	1.9	1.7139	3.3	0.1706	2.8	0.83	1015.2	26.1	1013.7	21.5	1010.5	37.8	1010.5	37.8
VMN17-34	48	4724	2.7	14.3618	3.9	1.5041	4.1	0.1567	1.2	0.29	938.2	10.3	932.0	25.1	917.4	81.0	938.2	10.3
VMN17-35	101	10276	3.0	12.8341	2.3	2.0986	2.5	0.1953	1.0	0.39	1150.2	10.5	1148.3	17.4	1144.8	46.2	1144.8	46.2
VMN17-36	253	15320	2.4	13.7389	1.0	1.5827	1.9	0.1577	1.6	0.83	944.0	13.8	963.4	11.7	1008.0	21.2	1008.0	21.2
VMN17-37	42	5010	0.8	10.8904	2.1	3.0184	5.8	0.2384	5.4	0.93	1378.4	66.5	1412.3	43.9	1463.7	39.8	1463.7	39.8
VMN17-38	98	14724	3.7	10.8966	1.0	3.0634	2.1	0.2421	1.9	0.88	1397.6	23.5	1423.6	16.2	1462.7	19.1	1462.7	19.1
VMN17-39	238	25380	4.8	13.2395	1.7	1.7813	2.7	0.1710	2.2	0.80	1017.9	20.6	1038.7	17.9	1082.7	33.4	1082.7	33.4
VMN17-40	112	7754	2.2	14.1789	2.1	1.5457	2.7	0.1590	1.7	0.61	951.0	14.8	948.8	16.7	943.7	43.9	951.0	14.8
VMN17-41	94	7672	4.6	13.7303	1.6	1.6271	1.9	0.1620	1.0	0.54	968.0	9.0	980.7	11.7	1009.2	32.0	1009.2	32.0
VMN17-42	312	48046	5.4	10.6199	1.6	3.1518	1.8	0.2428	1.0	0.54	1401.0	12.6	1445.4	14.2	1511.4	29.3	1511.4	29.3
VMN17-43	142	8780	3.2	16.4087	1.0	0.8462	1.7	0.1007	1.3	0.80	618.5	7.9	622.6	7.8	637.2	21.8	618.5	7.9
VMN17-44	173	17798	3.9	12.4280	1.1	2.2843	1.7	0.2059	1.3	0.76	1206.9	14.5	1207.4	12.3	1208.3	22.5	1208.3	22.5
VMN17-45	145	10646	2.4	14.2932	1.7	1.5277	2.0	0.1584	1.0	0.53	947.7	9.2	941.6	12.0	927.3	34.0	947.7	9.2
VMN17-46	297	23774	4.4	13.5888	1.0	1.6208	2.1	0.1597	1.8	0.87	955.3	16.1	978.3	13.0	1030.2	20.3	1030.2	20.3
VMN17-47	127	10246	2.8	13.8381	1.2	1.6522	1.8	0.1658	1.4	0.78	989.0	13.2	990.4	11.7	993.4	23.5	993.4	23.5
VMN17-48	85	7008	2.3	13.9921	1.8	1.6213	2.4	0.1645	1.6	0.64	981.9	14.1	978.5	15.1	970.8	37.6	970.8	37.6

DOI: 10.1344/105.000001698

Analysis	U (ppm)	^{206}Pb / ^{204}Pb	U/Th	$^{206}Pb^*$ / $^{207}Pb^*$	± (%)	Isotope ratios $^{207}Pb^*$ / $^{235}U^*$	± (%)	$^{206}Pb^*$ / ^{238}U	± (%)	error corr.	Apparent ages (Ma) $^{206}Pb^*$ / $^{238}U^*$	± (Ma)	$^{207}Pb^*$ / ^{235}U	± (Ma)	$^{206}Pb^*$ / $^{207}Pb^*$	± (Ma)	Best age (Ma)	± (Ma)
VMN17-49	218	13742	2.1	12.1049	1.2	1.6943	1.6	0.1488	1.2	0.70	894.0	9.6	1006.4	10.5	1260.0	22.9	1260.0	22.9
VMN17-50	148	19700	2.1	10.1057	1.0	3.8511	1.8	0.2823	1.5	0.83	1602.7	21.3	1603.5	14.5	1604.5	18.7	1604.5	18.7
VMN17-51	101	14754	1.6	11.4667	1.7	2.7946	1.9	0.2324	1.0	0.52	1347.1	12.2	1354.1	14.5	1365.1	31.9	1365.1	31.9
VMN17-52	138	18880	1.7	9.3416	1.8	4.3783	2.2	0.2966	1.3	0.58	1674.6	18.6	1708.3	18.1	1749.7	32.8	1749.7	32.8
VMN17-53	341	33630	5.4	12.4151	1.2	2.0381	1.6	0.1835	1.1	0.69	1086.2	11.1	1128.3	11.0	1210.4	23.0	1210.4	23.0
VMN17-54	43	3744	1.6	13.8669	3.6	1.6505	4.0	0.1660	1.8	0.45	990.0	16.5	989.7	25.5	989.1	73.4	989.1	73.4
VMN17-55	336	28072	2.0	14.2449	1.0	1.4652	2.3	0.1514	2.1	0.90	908.7	17.5	916.1	13.8	934.2	20.5	908.7	17.5
VMN17-56	30	3530	1.9	11.3769	3.7	2.9479	3.8	0.2432	1.0	0.26	1403.5	12.6	1394.3	28.9	1380.2	70.6	1380.2	70.6
VMN17-57	76	6854	3.2	13.9815	2.0	1.6077	2.3	0.1630	1.2	0.50	973.6	10.4	973.2	14.3	972.4	40.3	972.4	40.3
VMN17-58	149	12952	3.0	13.6284	1.7	1.7099	2.1	0.1690	1.3	0.61	1006.6	12.3	1012.2	13.8	1024.3	34.3	1024.3	34.3
VMN17-59	68	5716	2.7	14.2849	2.5	1.5385	2.7	0.1594	1.0	0.37	953.4	8.9	945.9	16.8	928.5	52.2	953.4	8.9
VMN17-60	179	15866	2.4	13.4252	1.5	1.8075	2.0	0.1760	1.3	0.66	1045.0	12.9	1048.2	13.4	1054.7	31.1	1054.7	31.1
VMN17-61	205	19684	4.6	13.5906	1.2	1.7334	1.6	0.1709	1.1	0.68	1016.8	10.5	1021.0	10.5	1030.0	24.1	1030.0	24.1
VMN17-62	56	5058	1.2	10.7941	2.8	3.3116	3.1	0.2593	1.4	0.45	1486.0	18.6	1483.8	24.4	1480.6	53.1	1480.6	53.1
VMN17-63	81	8652	3.9	12.7108	1.9	2.0555	3.5	0.1895	2.9	0.83	1118.6	29.6	1134.1	23.7	1163.9	38.4	1163.9	38.4
VMN17-64	241	16236	1.7	14.2124	1.0	1.4575	2.5	0.1502	2.3	0.92	902.3	19.6	913.0	15.3	938.9	20.7	902.3	19.6
VMN17-65	131	18144	1.5	10.4462	1.1	3.5095	1.7	0.2659	1.3	0.76	1519.9	17.9	1529.4	13.6	1542.4	20.9	1542.4	20.9
VMN17-66	174	22494	2.0	9.4063	4.1	4.2724	4.4	0.2915	1.7	0.38	1648.8	24.3	1688.1	36.3	1737.1	74.9	1737.1	74.9
VMN17-67	40	3622	2.0	13.8044	2.9	1.7450	3.1	0.1747	1.0	0.33	1038.0	9.6	1025.3	19.8	998.3	58.9	998.3	58.9
VMN17-69	134	11128	3.3	13.9543	1.8	1.6131	2.0	0.1633	1.0	0.49	974.8	9.0	975.3	12.8	976.3	36.2	976.3	36.2
VMN17-70	155	13398	3.8	13.7149	1.6	1.7019	1.9	0.1693	1.0	0.53	1008.2	9.3	1009.2	12.2	1011.5	32.9	1011.5	32.9
VMN17-71	75	7828	3.2	13.5219	1.2	1.7970	2.6	0.1762	2.3	0.88	1046.4	21.9	1044.4	16.9	1040.2	25.0	1040.2	25.0
VMN17-72	60	9514	1.1	9.1289	1.0	4.7247	1.4	0.3128	1.0	0.71	1754.6	15.4	1771.6	11.9	1791.8	18.2	1791.8	18.2
VMN17-73	85	13940	2.0	9.9234	2.0	4.1270	2.2	0.2970	1.0	0.45	1676.5	14.8	1659.7	18.4	1638.4	37.3	1638.4	37.3
VMN17-74	96	9514	3.1	13.8695	1.4	1.6092	1.9	0.1619	1.3	0.68	967.2	11.4	973.8	11.8	988.8	28.2	988.8	28.2
VMN17-75	85	7862	3.0	13.8852	2.1	1.6368	4.2	0.1648	3.7	0.87	983.6	33.8	984.5	26.7	986.5	42.0	986.5	42.0
VMN17-76	106	11792	6.5	13.6475	1.9	1.6635	2.1	0.1647	1.0	0.47	982.6	9.1	994.7	13.4	1021.5	37.8	1021.5	37.8
VMN17-77	245	21802	3.2	11.1807	2.0	2.4865	4.4	0.2016	3.9	0.89	1184.1	41.9	1268.1	31.6	1413.6	38.7	1413.6	38.7
VMN17-78	186	16582	2.6	14.1875	1.6	1.4637	1.9	0.1506	1.0	0.53	904.4	8.4	915.5	11.5	942.5	33.1	904.4	8.4
VMN17-79	212	21646	2.5	13.7366	1.1	1.5853	1.5	0.1579	1.0	0.69	945.3	8.8	964.4	9.1	1008.3	21.4	1008.3	21.4
VMN17-80	72	8190	1.9	11.1185	2.1	2.9946	2.3	0.2415	1.0	0.44	1394.4	12.5	1406.2	17.4	1424.2	39.4	1424.2	39.4
VMN17-81	462	25322	6.6	12.6367	1.5	1.7318	4.8	0.1587	4.6	0.95	949.6	40.4	1020.4	31.0	1175.5	29.1	1175.5	29.1
VMN17-82	48	4068	2.8	14.0894	2.5	1.6411	3.4	0.1677	2.3	0.68	999.4	21.1	986.1	21.3	956.7	50.9	956.7	50.9
VMN17-83	109	11350	3.2	12.6893	1.4	2.1176	1.7	0.1949	1.0	0.59	1147.8	10.5	1154.5	11.8	1167.3	27.4	1167.3	27.4
VMN17-84	79	13610	1.3	10.5591	1.2	3.3282	2.3	0.2549	1.9	0.85	1463.6	25.4	1487.7	17.9	1522.2	23.1	1522.2	23.1
VMN17-85	161	14324	1.2	14.3576	1.0	1.3848	3.0	0.1442	2.8	0.94	868.4	22.7	882.5	17.5	918.0	20.7	868.4	22.7
VMN17-86	111	11526	2.5	13.9427	1.5	1.6070	2.3	0.1625	1.7	0.75	970.7	15.5	972.9	14.3	978.0	30.8	978.0	30.8
VMN17-87	66	8440	1.3	11.6559	2.5	2.7453	3.1	0.2321	1.7	0.56	1345.4	21.0	1340.8	22.9	1333.5	49.2	1333.5	49.2
VMN17-88	107	10116	3.1	13.8168	1.5	1.6563	2.0	0.1660	1.3	0.66	989.9	11.8	992.0	12.4	996.5	30.1	996.5	30.1
VMN17-89	170	20486	0.9	11.6206	1.2	2.6982	2.3	0.2274	2.0	0.85	1320.9	23.3	1328.0	17.0	1339.4	23.4	1339.4	23.4
VMN17-90	51	4402	1.4	14.5388	3.2	1.4330	3.4	0.1511	1.0	0.30	907.1	8.5	902.8	20.2	892.2	66.5	907.1	8.5
VMN17-91	192	9742	2.1	7.4621	2.0	5.6396	2.9	0.3052	2.0	0.71	1717.1	30.5	1922.2	24.6	2151.2	35.3	2151.2	35.3
VMN17-92	37	3956	2.6	13.8406	2.2	1.6976	3.6	0.1704	2.8	0.79	1014.4	26.6	1007.6	22.8	993.0	44.4	993.0	44.4
VMN17-93	105	11276	3.7	13.6829	1.8	1.6274	3.0	0.1615	2.4	0.79	965.1	21.2	980.9	18.8	1016.3	37.1	1016.3	37.1
VMN17-94	106	9750	4.0	13.8029	1.6	1.6878	2.5	0.1690	2.0	0.77	1006.4	18.4	1003.9	16.2	998.5	32.7	998.5	32.7

DOI: 10.1344/105.000001698

Analysis	U (ppm)	^{206}Pb / ^{204}Pb	U/Th	$^{206}Pb^*$ / $^{207}Pb^*$	± (%)	Isotope ratios $^{207}Pb^*$ / $^{235}U^*$	± (%)	$^{206}Pb^*$ / ^{238}U	± (%)	error corr.	Apparent ages (Ma) $^{206}Pb^*$ / $^{238}U^*$	± (Ma)	$^{207}Pb^*$ / ^{235}U	± (Ma)	$^{206}Pb^*$ / $^{207}Pb^*$	± (Ma)	Best age (Ma)	± (Ma)
VMN17-95	326	34370	3.0	9.6363	1.2	3.4520	2.4	0.2413	2.0	0.86	1393.2	25.3	1516.3	18.6	1692.7	22.5	1692.7	22.5
VMN17-98	76	13608	1.6	9.0189	1.4	5.0185	1.7	0.3283	1.0	0.58	1830.0	15.9	1822.4	14.7	1813.8	25.8	1813.8	25.8
VMN18-1	143	12284	1.6	11.2946	2.4	2.5753	2.7	0.2110	1.2	0.43	1233.9	12.9	1293.7	19.5	1394.2	46.3	1394.2	46.3
VMN18-2	46	4864	0.5	10.6685	3.1	3.0557	4.7	0.2364	3.5	0.74	1368.1	42.9	1421.7	35.8	1502.7	59.0	1502.7	59.0
VMN18-3	131	9236	2.7	10.9675	2.6	2.9215	3.3	0.2324	2.0	0.60	1347.0	24.2	1387.5	24.9	1450.3	50.0	1450.3	50.0
VMN18-4	130	18370	2.0	10.6415	1.0	3.2138	1.4	0.2480	1.0	0.70	1428.4	12.8	1460.5	11.0	1507.5	19.2	1507.5	19.2
VMN18-5	97	13174	1.9	10.7126	1.2	3.1504	1.8	0.2448	1.3	0.73	1411.4	16.6	1445.1	13.8	1494.9	23.0	1494.9	23.0
VMN18-6	183	33798	2.3	8.0179	2.4	5.8047	2.8	0.3376	1.4	0.50	1874.9	22.3	1947.1	23.9	2024.8	42.3	2024.8	42.3
VMN18-7	40	5220	1.8	10.5880	3.4	3.1943	3.8	0.2453	1.6	0.41	1414.2	19.7	1455.8	29.2	1517.0	65.1	1517.0	65.1
VMN18-8	54	6916	1.8	10.5246	2.5	3.3583	3.2	0.2563	2.0	0.62	1471.1	25.9	1494.7	24.7	1528.4	46.6	1528.4	46.6
VMN18-9	71	2554	0.9	18.1797	5.2	0.6147	5.3	0.0810	1.0	0.19	502.4	4.8	486.5	20.7	412.5	117.4	502.4	4.8
VMN18-10	54	8774	1.2	9.0839	1.6	4.7601	1.9	0.3136	1.0	0.53	1758.4	15.4	1777.9	15.9	1800.8	29.2	1800.8	29.2
VMN18-11	95	12820	1.9	8.8527	1.8	4.9267	2.2	0.3163	1.4	0.63	1771.8	21.8	1806.8	19.0	1847.6	31.7	1847.6	31.7
VMN18-12	87	13760	1.3	8.1317	1.3	6.1679	1.6	0.3638	1.0	0.61	2000.0	17.2	1999.9	14.3	1999.8	23.1	1999.8	23.1
VMN18-13	79	8754	1.2	11.0015	1.2	2.9320	2.0	0.2339	1.6	0.80	1355.1	19.8	1390.2	15.3	1444.4	23.1	1444.4	23.1
VMN18-14	132	23378	1.2	8.8381	2.4	5.2035	2.7	0.3335	1.4	0.50	1855.5	22.1	1853.2	23.2	1850.5	42.5	1850.5	42.5
VMN18-15	195	24780	1.1	9.0011	1.2	4.7019	4.2	0.3070	4.0	0.95	1725.7	60.4	1767.6	35.0	1817.4	22.5	1817.4	22.5
VMN18-16	240	38882	1.7	9.0135	2.1	4.8872	3.5	0.3195	2.8	0.81	1787.2	44.3	1800.0	29.7	1814.9	37.8	1814.9	37.8
VMN18-17	290	7342	3.6	16.9432	3.1	0.6442	3.4	0.0792	1.4	0.42	491.1	6.7	504.9	13.5	567.8	67.0	491.1	6.7
VMN18-18	117	19694	1.4	8.2110	1.2	5.9271	1.6	0.3530	1.0	0.63	1948.8	16.8	1965.2	13.8	1982.6	21.9	1982.6	21.9
VMN18-19	97	16044	1.4	8.8337	2.2	4.8234	2.4	0.3090	1.0	0.42	1735.9	15.2	1789.0	20.1	1851.4	39.3	1851.4	39.3
VMN18-20	174	27470	1.7	8.4723	1.0	5.5698	2.1	0.3422	1.8	0.87	1897.5	30.1	1911.4	18.1	1926.6	18.7	1926.6	18.7
VMN18-21	66	9474	2.0	10.5232	1.6	3.2732	3.2	0.2498	2.8	0.86	1437.5	35.8	1474.7	25.1	1528.6	30.7	1528.6	30.7
VMN18-22	366	32066	3.0	10.2751	1.2	2.9161	2.7	0.2173	2.5	0.90	1267.7	28.2	1386.1	20.7	1573.4	22.9	1573.4	22.9
VMN18-23	87	11334	1.5	8.0347	1.7	6.1840	2.0	0.3604	1.1	0.54	1983.9	18.8	2002.2	17.9	2021.1	30.5	2021.1	30.5
VMN18-24	174	25190	2.1	10.9094	2.1	3.2326	2.3	0.2558	1.0	0.43	1468.2	13.1	1465.0	17.8	1460.4	39.4	1460.4	39.4
VMN18-25	215	34040	1.8	8.1837	1.0	5.8549	1.4	0.3475	1.0	0.71	1922.7	16.6	1954.6	12.3	1988.5	17.8	1988.5	17.8
VMN18-26	164	29672	2.0	8.4721	1.0	5.4037	1.5	0.3320	1.2	0.76	1848.2	18.6	1885.4	13.1	1926.7	17.9	1926.7	17.9
VMN18-27	202	31216	1.6	8.8638	1.0	4.9943	1.4	0.3211	1.0	0.71	1794.9	15.7	1818.4	12.0	1845.3	18.1	1845.3	18.1
VMN18-28	66	9828	1.8	11.1849	1.0	2.7367	2.1	0.2220	1.8	0.87	1292.5	21.0	1338.5	15.4	1412.9	19.9	1412.9	19.9
VMN18-29	94	19620	1.4	8.9448	1.5	5.0319	1.8	0.3264	1.0	0.57	1821.1	15.9	1824.7	14.9	1828.8	26.3	1828.8	26.3
VMN18-30	145	15762	1.4	10.7234	4.8	2.9623	6.0	0.2304	3.5	0.59	1336.6	42.5	1398.0	45.3	1493.0	91.2	1493.0	91.2
VMN18-31	101	15622	1.8	9.0192	2.0	4.7081	2.2	0.3080	1.1	0.47	1730.7	15.9	1768.7	18.6	1813.8	35.4	1813.8	35.4
VMN18-32	90	17128	1.2	7.5795	1.8	6.8542	2.0	0.3768	1.0	0.49	2061.2	17.6	2092.7	18.0	2123.9	31.0	2123.9	31.0
VMN18-33	134	17706	1.3	8.9094	2.1	4.4076	4.0	0.2848	3.5	0.86	1615.5	49.6	1713.8	33.5	1836.0	37.7	1836.0	37.7
VMN18-34	135	25996	1.4	8.1763	2.0	5.9752	2.5	0.3543	1.4	0.58	1955.2	24.1	1972.2	21.5	1990.1	35.9	1990.1	35.9
VMN18-36	103	13576	1.0	10.8332	1.5	3.2388	2.5	0.2545	2.1	0.81	1461.5	26.8	1466.5	19.7	1473.7	28.3	1473.7	28.3
VMN18-37	81	10164	0.6	10.7219	1.4	3.2225	2.1	0.2506	1.6	0.75	1441.5	20.0	1462.6	15.9	1493.3	25.6	1493.3	25.6
VMN18-38	187	34736	1.7	9.2098	1.0	4.5596	1.4	0.3046	1.0	0.71	1713.9	15.0	1741.9	11.8	1775.7	18.3	1775.7	18.3
VMN18-39	126	12306	1.9	11.1599	2.8	2.6055	7.1	0.2109	6.5	0.92	1233.5	73.1	1302.2	51.9	1417.1	52.6	1417.1	52.6
VMN18-40	151	16912	2.0	11.3098	1.7	2.8127	2.0	0.2307	1.1	0.54	1338.2	12.9	1358.9	14.9	1391.6	32.3	1391.6	32.3
VMN18-41	97	10064	1.6	9.0099	1.3	4.4578	1.7	0.2913	1.1	0.63	1648.0	15.7	1723.1	14.2	1815.7	24.0	1815.7	24.0
VMN18-42	206	20194	1.1	9.0535	1.4	4.0708	2.3	0.2673	1.8	0.78	1527.1	24.1	1648.5	18.4	1806.9	25.5	1806.9	25.5
VMN18-43	94	8326	1.0	10.8974	4.8	2.9370	8.9	0.2321	7.5	0.84	1345.6	90.6	1391.5	67.2	1462.5	90.9	1462.5	90.9
VMN18-44	117	25950	2.3	8.1595	1.8	5.9537	2.3	0.3523	1.4	0.61	1945.7	23.5	1969.1	20.1	1993.8	32.7	1993.8	32.7

DOI: 10.1344/105.000001698

Analysis	U (ppm)	^{206}Pb / ^{204}Pb	U/Th	$^{206}Pb^*$ / $^{207}Pb^*$	± (%)	Isotope ratios $^{207}Pb^*$ / $^{235}U^*$	± (%)	$^{206}Pb^*$ / ^{238}U	± (%)	error corr.	Apparent ages (Ma) $^{206}Pb^*$ / $^{238}U^*$	± (Ma)	$^{207}Pb^*$ / ^{235}U	± (Ma)	$^{206}Pb^*$ / $^{207}Pb^*$	± (Ma)	Best age (Ma)	± (Ma)
VMN18-45	113	14648	1.1	11.0982	2.4	3.0786	2.6	0.2478	1.0	0.38	1427.1	12.8	1427.4	20.0	1427.7	46.0	1427.7	46.0
VMN18-46	103	14530	2.5	11.0598	1.5	2.9869	2.9	0.2396	2.5	0.85	1384.6	31.1	1404.3	22.3	1434.4	29.3	1434.4	29.3
VMN18-47	196	17432	1.6	9.1023	1.5	4.4485	1.8	0.2937	1.0	0.55	1659.9	14.6	1721.4	15.0	1797.1	27.4	1797.1	27.4
VMN18-48	331	37606	1.5	8.9614	2.1	4.4729	2.8	0.2907	1.8	0.66	1645.1	26.3	1725.9	22.9	1825.4	37.7	1825.4	37.7
VMN18-49	214	31044	4.0	9.0714	1.5	4.6638	1.8	0.3068	1.1	0.59	1725.1	16.2	1760.8	15.1	1803.3	26.4	1803.3	26.4
VMN18-50	76	12400	1.0	9.1021	1.4	4.7706	1.9	0.3149	1.4	0.70	1764.9	21.2	1779.7	16.3	1797.1	25.2	1797.1	25.2
VMN18-51	93	10686	0.8	10.7904	2.0	3.3721	2.2	0.2639	1.0	0.45	1509.7	13.5	1497.9	17.3	1481.2	37.2	1481.2	37.2
VMN18-52	64	10382	2.5	10.6048	2.0	3.3584	2.3	0.2583	1.1	0.48	1481.2	14.6	1494.7	17.8	1514.1	37.5	1514.1	37.5
VMN18-53	86	18620	1.3	9.0737	1.8	4.6969	2.8	0.3091	2.1	0.76	1736.3	32.6	1766.7	23.5	1802.8	33.1	1802.8	33.1
VMN18-54	95	15428	2.0	9.0499	1.7	4.5993	4.9	0.3019	4.6	0.94	1700.6	69.4	1749.1	41.3	1807.6	31.3	1807.6	31.3
VMN18-55	180	27146	1.5	9.1933	2.1	4.4872	3.0	0.2992	2.2	0.71	1687.3	32.2	1728.6	25.3	1779.0	38.9	1779.0	38.9
VMN18-56	111	15588	2.1	10.8810	2.5	3.0806	2.8	0.2431	1.3	0.46	1402.9	16.1	1427.9	21.3	1465.4	46.9	1465.4	46.9
VMN18-57	110	18036	1.3	8.9097	2.4	4.5533	3.6	0.2942	2.7	0.76	1662.6	39.9	1740.8	29.9	1835.9	42.6	1835.9	42.6
VMN18-58	135	23186	1.6	9.0799	2.8	4.8282	3.3	0.3180	1.8	0.54	1779.7	27.5	1789.8	27.5	1801.6	50.0	1801.6	50.0
VMN18-59	224	25486	2.0	11.0744	1.4	2.9160	1.9	0.2342	1.3	0.67	1356.6	15.8	1386.1	14.6	1431.8	27.3	1431.8	27.3
VMN18-60	48	10040	1.1	8.1952	1.5	5.9291	1.8	0.3524	1.0	0.55	1946.1	16.8	1965.5	15.8	1986.0	27.1	1986.0	27.1
VMN18-61	258	33450	1.3	10.6096	1.6	3.2442	2.0	0.2496	1.2	0.62	1436.6	15.7	1467.8	15.4	1513.2	29.5	1513.2	29.5
VMN18-62	35	3862	0.8	12.6362	3.6	2.1851	3.7	0.2003	1.1	0.28	1176.7	11.3	1176.3	26.1	1175.6	71.2	1175.6	71.2
VMN18-63	204	24510	2.0	10.9314	1.9	3.0296	2.1	0.2402	1.0	0.47	1387.7	12.5	1415.1	16.3	1456.6	36.0	1456.6	36.0
VMN18-64	67	12158	1.5	7.5347	1.0	6.9989	1.4	0.3825	1.0	0.70	2087.8	17.8	2111.3	12.8	2134.2	18.0	2134.2	18.0
VMN18-65	245	31998	2.1	11.1044	1.0	2.8945	1.4	0.2331	1.0	0.71	1350.8	12.2	1380.5	10.7	1426.7	19.1	1426.7	19.1
VMN18-66	95	16638	1.5	10.8624	1.1	3.0140	2.9	0.2374	2.7	0.93	1373.4	33.5	1411.2	22.2	1468.6	20.0	1468.6	20.0
VMN18-67	97	20790	2.8	8.4921	1.7	5.3895	3.4	0.3319	2.9	0.86	1847.8	46.9	1883.2	28.9	1922.4	30.5	1922.4	30.5
VMN18-68	100	17992	2.5	11.1809	2.4	2.9198	2.7	0.2368	1.3	0.48	1369.9	15.9	1387.1	20.4	1413.5	45.4	1413.5	45.4
VMN18-69	286	16980	1.2	8.8675	2.8	3.7371	4.8	0.2403	3.9	0.82	1388.5	48.8	1579.4	38.4	1844.5	50.1	1844.5	50.1
VMN18-70	67	11448	1.3	8.0625	2.0	6.0014	2.2	0.3509	1.1	0.48	1939.0	18.1	1976.0	19.4	2015.0	34.6	2015.0	34.6
VMN18-71	51	10320	2.0	8.9704	2.2	5.0291	4.1	0.3272	3.5	0.85	1824.7	55.9	1824.2	35.0	1823.6	39.3	1823.6	39.3
VMN18-72	113	17842	1.5	9.0037	1.6	4.8074	1.8	0.3139	1.0	0.54	1760.0	15.4	1786.2	15.5	1816.9	28.2	1816.9	28.2
VMN18-73	110	16854	2.0	11.3504	1.1	2.7879	2.4	0.2295	2.2	0.89	1331.9	26.1	1352.3	18.1	1384.7	20.8	1384.7	20.8
VMN18-74	255	48104	2.8	8.1022	2.2	5.6858	2.4	0.3341	1.0	0.42	1858.3	16.1	1929.2	20.5	2006.3	38.2	2006.3	38.2
VMN18-75	84	11186	1.1	10.5210	3.0	3.2753	3.1	0.2499	1.0	0.32	1438.1	12.9	1475.2	24.5	1529.0	56.2	1529.0	56.2
VMN18-76	75	14134	1.3	8.2747	2.4	5.7466	3.6	0.3449	2.7	0.74	1910.1	44.0	1938.4	31.1	1968.8	43.2	1968.8	43.2
VMN18-77	134	16576	2.1	11.4151	1.6	2.7182	3.1	0.2250	2.7	0.86	1308.4	31.5	1333.4	23.0	1373.8	30.6	1373.8	30.6
VMN18-78	78	11698	2.6	11.2115	1.2	2.9043	3.8	0.2362	3.6	0.95	1366.7	44.8	1383.0	28.9	1408.3	22.7	1408.3	22.7
VMN18-79	91	16048	1.6	9.1128	1.0	4.6777	2.6	0.3092	2.4	0.92	1736.6	36.1	1763.3	21.5	1795.0	18.3	1795.0	18.3
VMN18-80	125	25090	1.8	9.1900	1.0	4.5814	3.9	0.3054	3.8	0.97	1717.8	57.6	1745.9	32.9	1779.6	18.3	1779.6	18.3
VMN18-81	259	15292	1.7	10.5800	1.6	2.7054	3.0	0.2076	2.6	0.86	1216.0	28.5	1329.9	22.3	1518.5	29.4	1518.5	29.4
VMN18-82	214	28832	2.8	11.1152	1.6	2.9145	1.9	0.2349	1.0	0.53	1360.4	12.8	1385.7	14.7	1424.8	31.5	1424.8	31.5
VMN18-83	143	21508	2.3	7.9633	1.9	5.9059	2.7	0.3411	1.8	0.68	1891.9	29.7	1962.1	23.1	2036.9	34.4	2036.9	34.4
VMN18-84	146	20450	1.7	8.2117	1.0	5.4879	2.3	0.3268	2.0	0.90	1823.1	32.4	1898.7	19.5	1982.4	17.8	1982.4	17.8
VMN18-85	48	6130	1.7	11.3255	1.6	2.8209	1.8	0.2317	1.0	0.54	1343.5	12.1	1361.1	13.8	1388.9	29.8	1388.9	29.8
VMN18-86	162	23928	1.5	9.1931	1.2	4.6396	1.9	0.3093	1.5	0.78	1737.5	22.5	1756.4	15.9	1779.0	21.9	1779.0	21.9
VMN18-87	50	8546	1.3	9.1122	1.3	4.7831	1.6	0.3161	1.0	0.62	1770.7	15.5	1781.9	13.6	1795.1	23.2	1795.1	23.2
VMN18-88	205	23092	1.0	9.0129	1.9	4.3908	3.5	0.2870	2.9	0.84	1626.6	42.1	1710.6	28.8	1815.0	34.0	1815.0	34.0
VMN18-89	147	23224	0.8	8.1394	1.0	6.0716	1.4	0.3584	1.0	0.71	1974.7	17.0	1986.2	12.3	1998.1	17.8	1998.1	17.8

DOI: 10.1344/105.000001698

Analysis	U (ppm)	^{206}Pb / ^{204}Pb	U/Th	$^{206}Pb^*$ / $^{207}Pb^*$	± (%)	Isotope ratios $^{207}Pb^*$ / $^{235}U^*$	± (%)	$^{206}Pb^*$ / ^{238}U	± (%)	error corr.	Apparent ages (Ma) $^{206}Pb^*$ / $^{238}U^*$	± (Ma)	$^{207}Pb^*$ / ^{235}U	± (Ma)	$^{206}Pb^*$ / $^{207}Pb^*$	± (Ma)	Best age (Ma)	± (Ma)
VMN18-90	141	23446	2.3	8.6722	2.0	4.5201	3.6	0.2843	3.0	0.83	1613.0	42.7	1734.7	29.9	1884.7	36.0	1884.7	36.0
VMN18-91	123	26542	2.0	8.2314	1.0	5.6817	1.4	0.3392	1.0	0.71	1882.8	16.3	1928.6	12.2	1978.1	17.8	1978.1	17.8
VMN18-92	127	15746	0.8	8.1872	1.0	5.0053	3.2	0.2972	3.1	0.95	1677.5	45.5	1820.2	27.4	1987.7	17.8	1987.7	17.8
VMN18-93	217	36166	2.0	9.0309	1.0	4.7603	1.6	0.3118	1.3	0.78	1749.5	19.2	1777.9	13.4	1811.4	18.2	1811.4	18.2
VMN18-94	65	5428	1.7	14.0318	3.0	1.6506	3.2	0.1680	1.0	0.32	1000.9	9.3	989.8	19.9	965.1	61.1	965.1	61.1
VMN18-95	82	15756	1.1	8.2249	1.1	6.0042	1.5	0.3582	1.0	0.67	1973.5	17.0	1976.5	13.1	1979.6	20.0	1979.6	20.0
VMN18-96	151	17188	2.0	10.9950	1.6	3.0397	1.9	0.2424	1.0	0.53	1399.1	12.6	1417.6	14.4	1445.6	30.5	1445.6	30.5
VMN18-97	119	19610	1.9	10.9373	2.0	3.2174	2.5	0.2552	1.5	0.59	1465.3	19.3	1461.4	19.4	1455.6	38.5	1455.6	38.5
VMN18-98	203	46448	2.6	8.0588	2.6	6.4344	2.8	0.3761	1.0	0.36	2057.9	17.6	2037.0	24.3	2015.8	45.8	2015.8	45.8
VMN18-99	117	17206	1.7	8.5278	2.0	5.2781	2.3	0.3264	1.0	0.45	1821.1	16.0	1865.3	19.4	1914.9	36.4	1914.9	36.4
VMN18-100	94	15970	1.3	8.9149	2.4	4.9359	2.6	0.3191	1.2	0.45	1785.5	18.7	1808.4	22.3	1834.9	42.6	1834.9	42.6
VMN32-1	113	13024	2.6	12.3770	1.1	2.3140	1.5	0.2077	1.0	0.68	1216.6	11.1	1216.6	10.4	1216.5	21.0	1216.5	21.0
VMN32-2	74	10328	2.3	11.0659	1.0	3.0921	2.3	0.2482	2.1	0.90	1429.0	27.0	1430.7	18.0	1433.3	19.4	1433.3	19.4
VMN32-3	345	22840	2.7	15.2761	1.1	1.1837	2.1	0.1311	1.8	0.86	794.4	13.8	793.0	11.7	789.2	22.7	794.4	13.8
VMN32-4	88	12898	2.3	10.9732	1.0	3.1213	1.5	0.2484	1.1	0.74	1430.3	14.0	1438.0	11.4	1449.3	19.1	1449.3	19.1
VMN32-5	127	22038	1.0	9.2231	1.0	4.7468	2.5	0.3175	2.2	0.91	1777.6	34.8	1775.5	20.6	1773.1	18.3	1773.1	18.3
VMN32-6	396	16026	3.1	10.3326	3.4	3.1140	3.5	0.2334	1.0	0.28	1352.1	12.2	1436.2	27.2	1563.0	63.6	1563.0	63.6
VMN32-7	32	5906	1.8	10.9443	1.6	3.1597	1.9	0.2508	1.0	0.53	1442.6	12.9	1447.4	14.6	1454.3	30.7	1454.3	30.7
VMN32-8	125	18284	1.1	10.7815	1.3	3.1467	1.6	0.2461	1.0	0.62	1418.1	12.7	1444.2	12.5	1482.8	24.1	1482.8	24.1
VMN32-9	68	14842	1.6	8.1747	1.6	5.8819	1.9	0.3487	1.0	0.53	1928.5	16.7	1958.6	16.2	1990.5	28.1	1990.5	28.1
VMN32-10	164	15290	2.7	13.7095	1.0	1.6974	1.4	0.1688	1.0	0.70	1005.3	9.3	1007.5	9.1	1012.3	20.7	1012.3	20.7
VMN32-10a	111	10706	2.5	13.9561	1.6	1.6699	1.9	0.1690	1.0	0.53	1006.8	9.3	997.2	12.0	976.1	32.7	976.1	32.7
VMN32-11	83	13240	0.9	10.5971	1.2	3.4293	1.5	0.2636	1.0	0.65	1508.1	13.4	1511.1	12.2	1515.4	22.3	1515.4	22.3
VMN32-12	73	9278	1.1	11.4039	1.5	2.8762	1.8	0.2379	1.0	0.56	1375.7	12.4	1375.7	13.5	1375.7	28.7	1375.7	28.7
VMN32-13	87	16410	2.3	9.4151	1.2	4.5846	2.0	0.3131	1.6	0.79	1755.7	24.4	1746.5	16.8	1735.4	22.6	1735.4	22.6
VMN32-15	46	7200	2.3	11.5627	2.4	2.8494	2.7	0.2390	1.2	0.44	1381.3	14.5	1368.7	20.0	1349.0	46.2	1349.0	46.2
VMN32-16	21	3304	0.6	10.9054	3.5	3.2639	3.7	0.2582	1.2	0.33	1480.4	16.3	1472.5	28.7	1461.1	66.2	1461.1	66.2
VMN32-17	75	10968	1.6	10.5663	1.6	3.2968	4.2	0.2526	3.9	0.92	1452.1	50.2	1480.3	32.7	1520.9	30.8	1520.9	30.8
VMN32-18	142	14562	3.2	13.7389	1.8	1.6675	2.0	0.1662	1.0	0.49	990.9	9.2	996.2	12.9	1008.0	36.0	1008.0	36.0
VMN32-20	29	4590	1.2	10.8795	1.1	3.2612	1.7	0.2573	1.2	0.73	1476.1	16.4	1471.8	13.1	1465.6	21.7	1465.6	21.7
VMN32-21	159	20314	2.6	12.6519	1.2	2.2098	1.6	0.2028	1.0	0.63	1190.2	10.9	1184.1	11.1	1173.1	24.4	1173.1	24.4
VMN32-22	57	8270	1.6	11.4692	2.9	2.8693	3.1	0.2387	1.0	0.33	1379.8	12.4	1373.9	23.1	1364.7	55.8	1364.7	55.8
VMN32-24	56	13870	1.5	9.0886	1.1	4.8525	2.1	0.3199	1.8	0.85	1789.1	28.1	1794.1	17.8	1799.8	20.1	1799.8	20.1
VMN32-25	113	10178	3.3	13.4775	1.3	1.7751	2.4	0.1735	2.0	0.85	1031.4	19.3	1036.4	15.5	1046.8	25.3	1046.8	25.3
VMN32-26	113	12146	1.9	11.1366	1.0	3.0596	1.8	0.2471	1.6	0.84	1423.6	19.8	1422.6	14.1	1421.1	19.1	1421.1	19.1
VMN32-27	104	19006	2.0	9.1005	1.0	4.8689	1.9	0.3214	1.6	0.84	1796.4	24.5	1796.9	15.6	1797.5	18.2	1797.5	18.2
VMN32-28	66	12828	1.4	9.1034	1.0	4.8181	1.4	0.3181	1.0	0.71	1780.5	15.6	1788.1	11.9	1796.9	18.2	1796.9	18.2
VMN32-29	68	7872	1.9	12.0883	1.7	2.4205	2.0	0.2122	1.0	0.50	1240.6	11.3	1248.7	14.5	1262.7	34.1	1262.7	34.1
VMN32-30	218	25208	1.5	9.0126	1.0	3.9639	7.8	0.2591	7.8	0.99	1485.3	103.2	1626.8	63.7	1815.1	18.7	1815.1	18.7
VMN32-31	183	18768	3.8	12.1301	2.2	2.3698	2.4	0.2085	1.0	0.42	1220.7	11.1	1233.5	17.1	1256.0	42.6	1256.0	42.6
VMN32-32	250	16450	1.2	8.1283	2.4	4.4323	3.7	0.2613	2.9	0.77	1496.5	38.6	1718.4	30.9	2000.6	41.9	2000.6	41.9
VMN32-33	77	11222	2.0	11.3270	1.1	2.8425	1.5	0.2335	1.0	0.66	1352.9	12.2	1366.8	11.4	1388.7	21.8	1388.7	21.8
VMN32-34	101	9216	1.5	13.9951	2.5	1.6283	2.6	0.1653	1.0	0.38	986.0	9.1	981.2	16.7	970.4	50.0	970.4	50.0
VMN32-36	90	23082	1.4	8.0171	1.9	6.2796	2.4	0.3651	1.6	0.64	2006.4	26.7	2015.6	21.1	2025.0	32.8	2025.0	32.8
VMN32-37	276	19852	1.5	10.3160	2.1	2.9497	5.4	0.2207	4.9	0.92	1285.5	57.5	1394.8	40.7	1566.0	39.5	1566.0	39.5

DOI: 10.1344/105.000001698

Analysis	U (ppm)	^{206}Pb / ^{204}Pb	U/Th	$^{206}Pb^*$ / $^{207}Pb^*$	± (%)	Isotope ratios $^{207}Pb^*$ / $^{235}U^*$	± (%)	$^{206}Pb^*$ / ^{238}U	± (%)	error corr.	Apparent ages (Ma) $^{206}Pb^*$ / $^{238}U^*$	± (Ma)	$^{207}Pb^*$ / ^{235}U	± (Ma)	$^{206}Pb^*$ / $^{207}Pb^*$	± (Ma)	Best age (Ma)	± (Ma)
VMN32-38	24	5812	2.6	8.3655	3.3	5.3935	4.5	0.3272	3.0	0.67	1825.0	47.4	1883.8	38.3	1949.3	59.6	1949.3	59.6
VMN32-39	172	35986	2.3	8.9442	1.0	4.6272	1.4	0.3002	1.0	0.70	1692.1	14.9	1754.2	12.0	1828.9	18.7	1828.9	18.7
VMN32-40	152	26992	1.1	8.0582	1.7	6.0441	2.0	0.3532	1.0	0.50	1950.0	16.8	1982.2	17.5	2015.9	30.9	2015.9	30.9
VMN32-14	559	31100	4.7	16.9882	1.2	0.7481	1.6	0.0922	1.0	0.63	568.4	5.4	567.1	6.9	562.1	26.8	568.4	5.4
VMN32-41	160	26612	1.1	8.1384	1.6	5.4647	2.7	0.3226	2.2	0.81	1802.2	34.6	1895.1	23.3	1998.4	28.1	1998.4	28.1
VMN32-42	127	5384	1.6	18.4203	4.2	0.5126	4.3	0.0685	1.0	0.23	427.0	4.1	420.2	14.9	383.0	94.7	427.0	4.1
VMN32-43	102	15298	1.2	10.5952	2.3	3.3581	2.5	0.2580	1.0	0.40	1479.8	13.2	1494.7	19.7	1515.8	43.6	1515.8	43.6
VMN32-44	136	23756	2.2	11.2281	1.3	3.0187	2.0	0.2458	1.6	0.78	1416.9	20.0	1412.4	15.4	1405.5	24.1	1405.5	24.1
VMN32-45	40	7032	1.1	10.6402	2.2	3.4217	3.2	0.2640	2.4	0.74	1510.5	32.5	1509.4	25.5	1507.8	40.9	1507.8	40.9
VMN32-46	479	39246	2.2	13.8805	1.7	1.6680	2.1	0.1679	1.3	0.60	1000.6	12.0	996.4	13.6	987.2	34.8	987.2	34.8
VMN32-47	25	4746	0.5	8.8749	1.8	5.1974	2.1	0.3345	1.0	0.48	1860.3	16.2	1852.2	17.7	1843.0	33.1	1843.0	33.1
VMN32-49	95	9778	0.7	10.9222	1.0	3.2271	1.4	0.2556	1.0	0.71	1467.5	13.1	1463.7	11.0	1458.2	19.1	1458.2	19.1
VMN32-51	156	30904	1.1	8.1394	1.4	6.2364	1.7	0.3681	1.0	0.58	2020.7	17.3	2009.6	15.1	1998.1	25.1	1998.1	25.1
VMN32-52	84	11722	1.0	9.0055	1.0	4.7113	1.4	0.3077	1.0	0.71	1729.4	15.2	1769.2	11.9	1816.5	18.2	1816.5	18.2
VMN32-53	211	39740	1.8	8.9886	1.0	4.9231	1.4	0.3209	1.0	0.71	1794.3	15.7	1806.2	11.9	1820.0	18.2	1820.0	18.2
VMN32-54	53	8404	1.2	10.6342	1.4	3.4797	1.7	0.2684	1.0	0.57	1532.6	13.6	1522.6	13.8	1508.8	27.1	1508.8	27.1
VMN32-55	115	17552	2.5	10.6956	1.2	3.3997	1.5	0.2637	1.0	0.66	1508.8	13.5	1504.3	12.0	1497.9	21.8	1497.9	21.8
VMN32-56	53	5700	1.6	12.9090	1.6	2.0426	2.4	0.1912	1.7	0.73	1128.1	17.9	1129.8	16.1	1133.2	32.0	1133.2	32.0
VMN32-57	51	6800	1.0	10.4631	1.9	3.4807	2.5	0.2641	1.5	0.62	1511.0	20.7	1522.8	19.5	1539.4	36.3	1539.4	36.3
VMN32-58	56	10004	1.3	8.9939	1.8	4.9915	2.0	0.3256	1.0	0.49	1817.0	15.8	1817.9	17.2	1818.9	32.2	1818.9	32.2
VMN32-59	121	17034	1.9	9.2001	1.0	4.2959	2.5	0.2866	2.3	0.92	1624.8	32.9	1692.6	20.6	1777.6	18.3	1777.6	18.3
VMN32-60	55	9150	1.4	10.6086	1.8	3.4824	2.4	0.2679	1.5	0.65	1530.3	20.7	1523.2	18.5	1513.4	33.8	1513.4	33.8
VMN32-61	129	25996	1.5	8.9669	1.6	4.8738	2.5	0.3170	1.9	0.77	1774.9	29.5	1797.7	20.8	1824.3	28.5	1824.3	28.5
VMN32-62	146	19502	2.2	10.2669	1.0	3.7360	1.5	0.2782	1.2	0.76	1582.3	16.4	1579.1	12.4	1574.9	18.8	1574.9	18.8
VMN32-63	73	9914	1.5	10.3069	2.1	3.4260	2.6	0.2561	1.6	0.62	1469.9	21.6	1510.4	20.7	1567.6	38.7	1567.6	38.7
VMN32-64	116	23458	2.1	9.1262	1.6	4.5645	2.4	0.3021	1.8	0.73	1701.8	26.3	1742.8	20.0	1792.3	29.7	1792.3	29.7
VMN32-65	73	14916	1.3	8.8302	1.3	5.2167	1.6	0.3341	1.0	0.62	1858.2	16.1	1855.3	13.9	1852.2	23.2	1852.2	23.2
VMN32-66	111	16876	2.0	11.1846	1.0	2.8491	3.0	0.2311	2.8	0.94	1340.3	33.6	1368.6	22.2	1412.9	19.2	1412.9	19.2
VMN32-67	221	57770	1.9	5.2963	1.6	13.7035	3.4	0.5264	3.0	0.88	2726.2	67.6	2729.4	32.6	2731.8	26.7	2731.8	26.7
VMN32-68	78	17510	1.7	9.0394	1.2	4.9407	1.6	0.3239	1.0	0.63	1808.8	15.8	1809.2	13.5	1809.7	22.6	1809.7	22.6
VMN32-69	84	11260	1.0	10.5311	1.1	3.4775	1.5	0.2656	1.0	0.69	1518.5	13.5	1522.1	11.5	1527.2	20.0	1527.2	20.0
VMN32-70	59	11734	1.7	8.8498	1.3	5.1569	1.6	0.3310	1.0	0.61	1843.2	16.0	1845.5	14.0	1848.1	23.6	1848.1	23.6
VMN32-71	74	15986	1.7	9.0280	1.1	4.9540	1.5	0.3244	1.0	0.68	1811.1	15.8	1811.5	12.4	1812.0	19.5	1812.0	19.5
VMN32-72	77	16418	1.8	9.2176	2.2	4.6670	2.4	0.3120	1.0	0.42	1750.5	15.3	1761.3	20.1	1774.2	40.0	1774.2	40.0
VMN32-73	243	29488	2.4	13.6854	1.8	1.7025	2.5	0.1690	1.7	0.69	1006.5	16.2	1009.5	16.0	1015.9	36.5	1015.9	36.5
VMN32-74	32	5562	1.3	10.6296	1.4	3.4764	1.7	0.2680	1.0	0.61	1530.7	14.2	1521.9	13.5	1509.6	25.6	1509.6	25.6
VMN32-75	150	28750	1.9	8.9593	1.0	4.9962	1.4	0.3246	1.0	0.71	1812.4	15.8	1818.7	12.0	1825.9	18.1	1825.9	18.1
VMN32-76	93	20332	115.4	7.9805	1.6	6.4241	1.9	0.3718	1.0	0.53	2038.0	17.5	2035.6	16.7	2033.1	28.5	2033.1	28.5
VMN32-77	56	8060	0.8	10.5410	1.2	3.4768	1.6	0.2658	1.0	0.63	1519.4	13.5	1522.0	12.5	1525.4	23.1	1525.4	23.1
VMN32-78	89	14666	2.1	10.2043	1.4	3.7646	1.7	0.2786	1.0	0.59	1584.4	14.0	1585.2	13.6	1586.4	25.5	1586.4	25.5
VMN32-79	63	4864	2.6	13.4003	1.8	1.7376	2.3	0.1689	1.4	0.62	1005.9	13.0	1022.6	14.6	1058.4	36.0	1058.4	36.0
VMN32-80	216	16324	1.9	11.2762	1.6	2.6805	2.4	0.2192	1.8	0.74	1277.7	20.5	1323.1	17.6	1397.3	30.7	1397.3	30.7
VMN32-81	101	11744	3.2	14.1633	2.2	1.5721	2.4	0.1615	1.0	0.42	965.1	9.0	959.3	14.8	946.0	44.5	965.1	9.0
VMN32-82	305	22362	2.1	14.2950	1.5	1.4608	2.3	0.1515	1.7	0.74	909.1	14.3	914.3	13.8	927.0	31.7	909.1	14.3
VMN32-83	50	10456	2.0	8.2680	1.1	6.0199	1.5	0.3610	1.0	0.68	1986.8	17.1	1978.7	12.8	1970.3	19.3	1970.3	19.3

DOI: 10.1344/105.000001698

Analysis	U (ppm)	$^{206}Pb/^{204}Pb$	U/Th	$^{206}Pb^*/^{207}Pb^*$	± (%)	Isotope ratios $^{207}Pb^*/^{235}U^*$	± (%)	$^{206}Pb^*/^{238}U$	± (%)	error corr.	Apparent ages (Ma) $^{206}Pb^*/^{238}U^*$	± (Ma)	$^{207}Pb^*/^{235}U$	± (Ma)	$^{206}Pb^*/^{207}Pb^*$	± (Ma)	Best age (Ma)	± (Ma)
VMN32-84	171	12938	0.9	13.8297	2.2	1.6493	2.4	0.1654	1.0	0.42	986.9	9.2	989.3	15.2	994.6	44.3	994.6	44.3
VMN32-85	340	26616	3.7	13.8909	1.4	1.5887	1.7	0.1601	1.0	0.59	957.1	8.9	965.8	10.6	985.6	27.9	985.6	27.9
VMN32-86	64	10520	2.1	11.3544	1.9	2.9331	2.2	0.2415	1.0	0.46	1394.7	12.5	1390.5	16.3	1384.0	36.7	1384.0	36.7
VMN32-87	69	7552	3.8	13.8848	1.5	1.6862	1.8	0.1698	1.0	0.54	1011.1	9.4	1003.3	11.7	986.5	31.4	986.5	31.4
VMN32-88	123	20132	1.3	10.3865	1.4	3.6391	1.7	0.2741	1.0	0.59	1561.7	13.9	1558.1	13.5	1553.2	25.7	1553.2	25.7
VMN32-89	94	14302	2.0	11.1958	1.1	2.9782	1.6	0.2418	1.1	0.68	1396.2	13.3	1402.1	11.9	1411.0	21.9	1411.0	21.9
VMN32-90	67	4672	1.1	16.8824	3.4	0.7668	3.6	0.0939	1.4	0.38	578.5	7.7	577.9	16.1	575.7	73.2	578.5	7.7
VMN32-91	99	19378	1.6	8.9642	1.0	5.0277	1.4	0.3269	1.0	0.71	1823.2	15.9	1824.0	12.0	1824.9	18.1	1824.9	18.1
VMN32-92	42	9416	1.6	9.1497	1.4	4.8412	2.0	0.3213	1.4	0.71	1795.9	22.1	1792.1	16.7	1787.6	25.4	1787.6	25.4
VMN32-93	82	8828	0.9	10.2979	2.1	3.6697	2.8	0.2741	1.9	0.67	1561.5	25.8	1564.8	22.2	1569.3	38.6	1569.3	38.6
VMN32-94	83	17234	1.3	8.2557	1.5	5.9507	2.0	0.3563	1.4	0.69	1964.6	23.7	1968.7	17.5	1972.9	25.8	1972.9	25.8
VMN32-95	79	13784	2.3	11.0779	1.4	3.0740	2.2	0.2470	1.7	0.78	1422.9	22.1	1426.2	17.1	1431.2	26.9	1431.2	26.9
VMN32-96	111	16540	2.2	10.6406	1.4	3.3436	1.9	0.2580	1.4	0.71	1479.8	17.8	1491.3	14.9	1507.7	25.5	1507.7	25.5
VMN32-97	155	7890	2.2	16.6829	1.5	0.8144	1.8	0.0985	1.0	0.55	605.9	5.8	604.9	8.3	601.4	33.1	605.9	5.8
VMN32-98	116	4908	1.1	17.6897	2.3	0.6152	2.5	0.0789	1.0	0.40	489.7	4.7	486.8	9.7	473.2	51.2	489.7	4.7
VMN32-99	163	31680	2.4	7.8002	1.3	6.2472	1.7	0.3534	1.0	0.60	1950.9	16.8	2011.1	14.5	2073.4	23.3	2073.4	23.3
VMN32-100	87	7866	2.4	13.7933	1.5	1.5831	1.8	0.1584	1.0	0.55	947.7	8.8	963.6	11.3	1000.0	30.7	1000.0	30.7
VMN35-1	39	3936	2.5	12.6549	2.5	2.2148	3.0	0.2033	1.5	0.52	1192.9	16.7	1185.7	20.7	1172.6	50.3	1172.6	50.3
VMN35-2	46	1642	1.5	16.6669	6.5	0.7245	6.6	0.0876	1.1	0.17	541.2	5.7	553.3	28.0	603.5	140.4	541.2	5.7
VMN35-3	115	13330	0.8	8.8906	1.6	4.8178	1.9	0.3107	1.0	0.54	1743.9	15.3	1788.0	15.6	1839.8	28.3	1839.8	28.3
VMN35-4	223	26040	2.5	9.1266	1.3	4.0207	1.6	0.2661	1.0	0.64	1521.2	14.1	1638.4	13.3	1792.3	23.0	1792.3	23.0
VMN35-5	81	9682	1.2	11.2410	2.1	3.0290	2.5	0.2469	1.4	0.54	1422.7	17.5	1415.0	19.3	1403.3	40.7	1403.3	40.7
VMN35-6	47	4014	1.7	14.3164	2.8	1.5166	3.3	0.1575	1.7	0.52	942.7	15.3	937.1	20.4	923.9	58.4	942.7	15.3
VMN35-7	156	18208	1.4	8.1537	1.0	4.9549	2.1	0.2930	1.8	0.87	1656.6	26.4	1811.7	17.5	1995.0	18.0	1995.0	18.0
VMN35-8	270	33926	3.4	11.6910	1.5	2.6293	1.9	0.2229	1.3	0.65	1297.4	14.9	1308.9	14.3	1327.7	28.5	1327.7	28.5
VMN35-9	102	11960	1.6	9.0280	2.8	3.8601	6.2	0.2527	5.5	0.89	1452.6	71.8	1605.4	49.9	1812.0	50.7	1812.0	50.7
VMN35-10	159	10702	2.9	13.4414	3.4	1.4761	4.2	0.1439	2.4	0.58	866.7	19.5	920.6	25.2	1052.2	68.4	866.7	19.5
VMN35-11	74	11656	2.0	9.6719	1.3	3.9821	2.2	0.2793	1.8	0.80	1588.0	24.8	1630.6	17.8	1685.9	24.1	1685.9	24.1
VMN35-12	68	9476	3.3	10.7183	1.2	3.1157	2.1	0.2422	1.8	0.84	1398.1	22.4	1436.6	16.4	1493.9	22.1	1493.9	22.1
VMN35-13	113	9868	2.0	12.4898	1.1	2.1891	1.5	0.1983	1.1	0.69	1166.2	11.3	1177.6	10.8	1198.6	22.2	1198.6	22.2
VMN35-14	117	20810	1.5	8.9152	1.8	4.7654	3.1	0.3081	2.5	0.82	1731.5	38.6	1778.8	25.9	1834.8	31.9	1834.8	31.9
VMN35-15	197	30504	1.4	8.8958	1.6	4.8796	5.1	0.3148	4.8	0.95	1764.4	74.4	1798.7	42.9	1838.8	29.5	1838.8	29.5
VMN35-16	167	26810	2.7	9.1372	1.0	4.4867	1.4	0.2973	1.0	0.71	1678.0	14.8	1728.5	11.7	1790.1	18.2	1790.1	18.2
VMN35-17	358	45606	3.8	11.2841	1.3	2.9591	3.3	0.2422	3.1	0.92	1398.0	38.6	1397.2	25.4	1395.9	25.7	1395.9	25.7
VMN35-18	80	10870	1.9	11.1894	2.4	2.8550	2.6	0.2317	1.0	0.38	1343.4	12.1	1370.1	19.9	1412.1	46.7	1412.1	46.7
VMN35-20	170	11872	2.2	13.5598	2.1	1.7297	2.3	0.1701	1.0	0.44	1012.7	9.4	1019.6	14.7	1034.5	41.5	1034.5	41.5
VMN35-21	34	1502	1.2	18.8217	7.6	0.5477	7.7	0.0748	1.1	0.14	464.8	4.7	443.5	27.7	334.3	173.4	464.8	4.7
VMN35-22	167	30424	1.3	8.9971	1.0	4.7701	2.4	0.3113	2.1	0.91	1746.9	32.6	1779.7	19.8	1818.2	18.2	1818.2	18.2
VMN35-23	98	10674	1.9	11.1910	2.3	2.7731	5.4	0.2251	4.9	0.91	1308.7	57.7	1348.3	40.1	1411.8	43.1	1411.8	43.1
VMN35-24	286	43822	2.3	10.5872	1.3	3.3014	1.6	0.2535	1.0	0.62	1456.5	13.0	1481.4	12.5	1517.2	23.6	1517.2	23.6
VMN35-25	282	20626	1.0	9.2839	1.2	3.5459	6.1	0.2388	5.9	0.98	1380.2	73.7	1537.5	48.0	1761.1	22.3	1761.1	22.3
VMN35-26	243	20028	3.3	13.6552	1.2	1.7662	1.8	0.1749	1.4	0.76	1039.2	13.4	1033.1	11.9	1020.4	23.9	1020.4	23.9
VMN35-27	126	5968	1.1	17.8758	4.2	0.6646	4.3	0.0862	1.1	0.25	532.8	5.5	517.4	17.5	450.0	93.1	532.8	5.5
VMN35-28	129	24002	1.0	8.5969	1.0	5.4992	1.5	0.3429	1.1	0.74	1900.5	18.3	1900.5	12.8	1900.4	18.0	1900.4	18.0
VMN35-29	155	19734	1.6	8.8645	1.1	5.1214	2.6	0.3293	2.4	0.90	1834.8	37.8	1839.7	22.3	1845.2	20.5	1845.2	20.5

DOI: 10.1344/105.000001698

Analysis	U (ppm)	^{206}Pb ^{204}Pb	U/Th	$^{206}Pb^*$ $^{207}Pb^*$	± (%)	Isotope ratios $^{207}Pb^*$ $^{235}U^*$	± (%)	$^{206}Pb^*$ ^{238}U	± (%)	error corr.	Apparent ages (Ma) $^{206}Pb^*$ $^{238}U^*$	± (Ma)	$^{207}Pb^*$ ^{235}U	± (Ma)	$^{206}Pb^*$ $^{207}Pb^*$	± (Ma)	Best age (Ma)	± (Ma)
VMN35-30	123	6048	1.8	17.2466	3.5	0.6246	3.9	0.0781	1.8	0.46	485.0	8.3	492.7	15.2	529.1	76.2	485.0	8.3
VMN35-32	289	24568	3.1	13.4925	2.2	1.8614	2.6	0.1822	1.5	0.57	1078.7	15.0	1067.5	17.4	1044.6	43.4	1044.6	43.4
VMN35-33	115	18484	1.2	8.9679	1.3	4.7469	2.2	0.3087	1.7	0.80	1734.5	26.5	1775.6	18.1	1824.1	23.3	1824.1	23.3
VMN35-34	48	6694	0.9	10.3684	1.5	3.6607	1.8	0.2753	1.0	0.56	1567.5	13.9	1562.8	14.1	1556.5	27.4	1556.5	27.4
VMN35-35	86	14290	1.5	8.6550	1.8	5.4298	2.3	0.3408	1.5	0.66	1890.7	25.2	1889.6	20.1	1888.3	31.7	1888.3	31.7
VMN35-36	149	25796	2.1	8.6373	1.1	5.4212	1.6	0.3396	1.2	0.73	1884.8	19.0	1888.2	13.6	1892.0	19.6	1892.0	19.6
VMN35-37	296	31526	2.1	8.0874	1.1	4.6566	2.8	0.2731	2.5	0.92	1556.7	35.1	1759.5	23.0	2009.5	19.0	2009.5	19.0
VMN35-39	145	24910	1.7	8.8354	1.4	5.1577	3.0	0.3305	2.7	0.88	1840.8	42.4	1845.7	25.5	1851.1	25.3	1851.1	25.3
VMN35-40	164	23970	1.2	8.9805	1.0	5.0184	2.0	0.3269	1.7	0.86	1823.2	27.3	1822.4	16.9	1821.6	18.2	1821.6	18.2
VMN35-41	125	10552	2.5	14.1137	1.5	1.5128	2.1	0.1548	1.5	0.69	928.1	12.5	935.6	12.8	953.2	30.7	928.1	12.5
VMN35-42	82	12136	4.1	12.9771	1.9	2.0310	2.2	0.1912	1.0	0.46	1127.6	10.3	1126.0	14.8	1122.7	38.5	1122.7	38.5
VMN35-43	594	56202	2.2	13.6907	1.7	1.6715	2.8	0.1660	2.2	0.79	989.9	20.3	997.8	17.7	1015.1	34.3	1015.1	34.3
VMN35-44	159	12660	3.2	13.6458	1.2	1.6777	2.0	0.1660	1.6	0.81	990.2	14.8	1000.1	12.7	1021.8	23.8	1021.8	23.8
VMN35-45	129	16600	1.9	11.4426	2.1	2.9038	2.6	0.2410	1.6	0.59	1391.8	19.4	1382.9	19.8	1369.1	40.8	1369.1	40.8
VMN35-46	148	14108	1.8	12.0148	1.5	2.5663	2.2	0.2236	1.6	0.73	1301.0	18.6	1291.1	15.8	1274.6	28.7	1274.6	28.7
VMN35-47	146	22942	1.4	9.0671	1.1	4.9099	1.5	0.3229	1.0	0.67	1803.8	15.7	1804.0	12.6	1804.2	20.2	1804.2	20.2
VMN35-48	84	18350	1.6	9.1032	1.4	4.7112	1.7	0.3110	1.0	0.58	1745.9	15.3	1769.2	14.4	1796.9	25.3	1796.9	25.3
VMN35-49	127	11800	4.7	13.7126	1.3	1.5933	1.7	0.1585	1.0	0.62	948.2	9.2	967.6	10.5	1011.9	26.7	1011.9	26.7
VMN35-50	73	10810	5.3	10.7909	1.5	3.2806	2.2	0.2567	1.7	0.74	1473.2	21.7	1476.5	17.2	1481.2	28.0	1481.2	28.0
VMN35-51	139	20828	1.3	10.4330	1.9	3.3967	2.5	0.2570	1.7	0.68	1474.6	22.8	1503.6	19.9	1544.8	35.0	1544.8	35.0
VMN35-52	93	13862	1.3	8.9111	2.1	4.9816	2.4	0.3220	1.1	0.46	1799.3	17.3	1816.2	20.3	1835.6	38.6	1835.6	38.6
VMN35-53	39	6240	1.6	10.9515	2.6	3.2591	3.4	0.2589	2.2	0.64	1484.0	29.2	1471.4	26.7	1453.1	50.1	1453.1	50.1
VMN35-54	94	12092	1.6	10.5291	2.1	3.5455	2.6	0.2707	1.5	0.56	1544.6	20.1	1537.4	20.5	1527.6	40.2	1527.6	40.2
VMN35-55	119	11494	2.8	13.3034	1.1	1.8727	1.5	0.1807	1.0	0.67	1070.7	9.9	1071.5	9.8	1073.0	22.0	1073.0	22.0
VMN35-56	194	25238	1.4	9.3108	1.0	4.3801	1.8	0.2958	1.5	0.83	1670.3	21.6	1708.6	14.7	1755.8	18.3	1755.8	18.3
VMN35-57	85	15096	0.9	8.7025	1.2	5.3302	1.8	0.3364	1.4	0.75	1869.4	22.4	1873.7	15.8	1878.4	22.0	1878.4	22.0
VMN35-58	48	5964	2.4	12.6933	2.7	2.1886	3.0	0.2015	1.3	0.42	1183.3	13.6	1177.4	20.7	1166.6	53.3	1166.6	53.3
VMN35-59	188	23462	2.2	12.2902	1.8	2.3092	2.4	0.2058	1.6	0.68	1206.6	18.0	1215.1	17.1	1230.3	34.8	1230.3	34.8
VMN35-60	142	19226	2.2	10.7099	1.3	3.3745	1.6	0.2621	1.0	0.61	1500.7	13.4	1498.5	12.9	1495.4	24.6	1495.4	24.6
VMN35-61	77	9592	1.3	10.7457	1.4	3.1803	3.2	0.2479	2.8	0.89	1427.4	36.1	1452.4	24.4	1489.1	27.1	1489.1	27.1
VMN35-62	196	26998	3.3	10.3521	1.1	3.5856	1.5	0.2692	1.0	0.67	1536.8	13.7	1546.3	11.9	1559.4	21.0	1559.4	21.0
VMN35-63	196	19894	1.6	12.3848	1.0	2.3257	1.5	0.2089	1.2	0.76	1222.9	13.1	1220.2	11.0	1215.2	19.7	1215.2	19.7
VMN35-64	147	15636	2.3	12.1129	1.3	2.4306	1.6	0.2135	1.0	0.62	1247.6	11.3	1251.7	11.6	1258.7	24.6	1258.7	24.6
VMN35-65	148	18164	1.0	9.1492	1.7	4.7188	2.3	0.3131	1.6	0.70	1756.1	24.9	1770.6	19.4	1787.8	30.1	1787.8	30.1
VMN35-66	79	11658	2.1	10.7872	1.5	3.2874	1.9	0.2572	1.0	0.55	1475.5	13.5	1478.1	14.4	1481.8	29.3	1481.8	29.3
VMN35-67	80	3374	1.2	16.9458	2.4	0.7771	2.7	0.0955	1.1	0.40	588.0	6.0	583.8	11.8	567.5	53.3	588.0	6.0
VMN35-68	169	17480	2.8	12.6762	1.3	2.1985	2.4	0.2021	2.0	0.84	1186.7	22.0	1180.6	16.8	1169.3	25.6	1169.3	25.6
VMN35-69	68	13292	1.4	8.2427	1.0	5.9467	1.5	0.3555	1.1	0.73	1960.8	18.9	1968.1	13.3	1975.7	18.4	1975.7	18.4
VMN35-70	52	7834	1.2	10.9408	1.5	3.1675	2.1	0.2513	1.5	0.72	1445.4	19.6	1449.3	16.2	1455.0	27.7	1455.0	27.7
VMN35-71	150	19758	0.9	8.7383	1.0	5.3219	1.4	0.3373	1.0	0.71	1873.6	16.3	1872.4	12.1	1871.1	18.1	1871.1	18.1
VMN35-72	157	18628	2.0	9.9407	1.0	3.9714	1.4	0.2863	1.0	0.71	1623.1	14.3	1628.4	11.5	1635.1	18.6	1635.1	18.6
VMN35-73	86	10312	1.2	11.2792	1.8	3.0074	2.1	0.2460	1.1	0.52	1417.9	13.7	1409.5	15.9	1396.8	34.1	1396.8	34.1
VMN35-74	97	12848	0.9	10.1012	1.3	3.8417	1.6	0.2814	1.0	0.62	1598.6	14.2	1601.5	12.9	1605.3	23.3	1605.3	23.3
VMN35-75	67	6474	1.6	12.3271	1.9	2.4110	2.2	0.2156	1.0	0.46	1258.3	11.4	1245.9	15.5	1224.4	37.6	1224.4	37.6
VMN35-77	217	25090	2.0	10.8724	1.3	3.2429	1.6	0.2557	1.0	0.62	1467.9	13.1	1467.5	12.5	1466.9	23.9	1466.9	23.9

DOI: 10.1344/105.000001698

Analysis	U (ppm)	^{206}Pb ^{204}Pb	U/Th	$^{206}Pb^*$ $^{207}Pb^*$	± (%)	Isotope ratios $^{207}Pb^*$ $^{235}U^*$	± (%)	$^{206}Pb^*$ ^{238}U	± (%)	error corr.	Apparent ages (Ma) $^{206}Pb^*$ $^{238}U^*$	± (Ma)	$^{207}Pb^*$ ^{235}U	± (Ma)	$^{206}Pb^*$ $^{207}Pb^*$	± (Ma)	Best age (Ma)	± (Ma)
VMN35-78	180	20142	0.8	10.3994	1.0	3.5695	1.8	0.2692	1.5	0.82	1536.9	19.8	1542.8	14.0	1550.9	18.8	1550.9	18.8
VMN35-80	110	2886	1.5	11.3766	4.6	2.6466	4.9	0.2184	1.7	0.35	1273.3	19.8	1313.7	35.9	1380.3	87.5	1380.3	87.5
VMN35-81	31	2972	2.1	13.9961	3.3	1.6628	3.6	0.1688	1.4	0.40	1005.4	13.3	994.4	22.7	970.3	67.1	970.3	67.1
VMN35-82	106	10362	1.9	13.8472	1.9	1.6541	2.8	0.1661	2.0	0.73	990.7	18.4	991.1	17.5	992.0	38.6	992.0	38.6
VMN35-83	509	45892	3.7	10.3142	1.6	3.7371	3.4	0.2796	3.0	0.89	1589.1	42.4	1579.4	27.2	1566.3	29.6	1566.3	29.6
VMN35-84	133	32152	3.3	7.0779	1.4	7.9676	2.2	0.4090	1.8	0.78	2210.4	32.7	2227.4	20.2	2243.0	24.2	2243.0	24.2
VMN35-85	112	19220	1.1	7.8639	1.0	6.6605	1.4	0.3799	1.0	0.71	2075.7	17.7	2067.4	12.5	2059.1	17.7	2059.1	17.7
VMN35-86	148	11418	1.7	13.3320	2.2	1.8969	2.4	0.1834	1.1	0.45	1085.6	10.9	1080.0	16.2	1068.7	43.9	1068.7	43.9
VMN35-87	103	11484	1.5	12.3783	1.2	2.3118	1.6	0.2075	1.0	0.65	1215.7	11.1	1215.9	11.0	1216.2	23.3	1216.2	23.3
VMN35-88	190	25886	2.3	10.1803	1.3	3.8143	1.7	0.2816	1.1	0.64	1599.5	15.6	1595.8	13.8	1590.8	24.7	1590.8	24.7
VMN35-89	182	35642	2.8	9.2022	1.2	4.4845	1.8	0.2993	1.4	0.74	1687.8	20.3	1728.1	15.3	1777.2	22.4	1777.2	22.4
VMN35-90	531	77414	6.1	10.4036	1.6	3.5754	2.7	0.2698	2.2	0.80	1539.7	29.7	1544.1	21.5	1550.1	30.4	1550.1	30.4
VMN35-91	13	1556	1.1	11.0833	1.6	3.1392	2.3	0.2523	1.8	0.75	1450.5	22.7	1442.4	18.0	1430.3	29.6	1430.3	29.6
VMN35-92	56	5028	1.8	13.5824	2.3	1.8269	2.5	0.1800	1.0	0.39	1066.8	9.8	1055.2	16.7	1031.2	47.3	1031.2	47.3
VMN35-93	55	7704	0.6	7.1906	1.2	6.5398	1.5	0.3411	1.0	0.65	1891.7	16.4	2051.3	13.5	2215.7	20.2	2215.7	20.2
VMN35-95	61	6058	1.7	13.1500	2.0	1.9852	2.4	0.1893	1.4	0.56	1117.8	14.1	1110.5	16.4	1096.3	40.3	1096.3	40.3
VMN35-96	169	39042	4.5	8.4099	2.2	5.6463	3.7	0.3444	3.0	0.80	1907.8	49.0	1923.2	31.9	1939.9	39.4	1939.9	39.4
VMN35-97	199	31920	2.3	9.0972	1.4	4.6383	1.8	0.3060	1.1	0.62	1721.1	16.6	1756.2	14.8	1798.1	25.3	1798.1	25.3
VMN35-99	146	17330	4.7	13.5798	1.5	1.6912	2.1	0.1666	1.4	0.67	993.1	12.9	1005.2	13.3	1031.6	31.2	1031.6	31.2
VMN35-100	45	6718	1.7	10.6844	2.9	3.3770	3.9	0.2617	2.6	0.66	1498.5	34.1	1499.1	30.5	1499.9	55.5	1499.9	55.5

DOI: 10.1344/105.000001698